

Lecture note on solid state physics

Superexchange interaction

Masatsugu Suzuki and Itsuko S. Suzuki
Department of Physics, State University of New York at Binghamton
Binghamton, New York 13902-6000, U.S.A.
(August 8, 2007, revised May 28, 2009)

Abstract

In preparing this note, we have examined many textbooks of magnetism where the mechanism of the superexchange interaction is discussed. We realize that it may be difficult for readers (in particular graduate students and undergraduate students studying on the magnetism) to understand the physics on the superexchange interactions from these textbooks, partly because of the limited space of the textbooks and the requirement of the amount of knowledge in quantum mechanics. The present note is based on the lecture note of the Solid State Physics which one of the authors (MS) has prepared since 1986. The note has been revised many times. The Mathematica programs are used for calculations of the eigenvalue problems and plotting the electronic density of the wavefunctions. The use of the Mathematica will be helpful for students to understand the mechanism of the superexchange interactions visually. As a supplementary, one can see our lecture note on the spin Hamiltonian and the crystal field of transition metal ions.

In this note, we discuss the development of various interactions between magnetic ions; such as direct exchange interaction and superexchange interaction. Direct exchange involves an overlap of electron wavefunctions from the two sites and Coulomb electrostatic interaction repulsion. The Pauli exclusion principle keeps the electrons with parallel spin away from each other, thereby reducing the Coulomb repulsion. Originally superexchange acquired its name because of the relatively large distances, occupied by normally diamagnetic ions, radicals, or molecules. Small exchange coupling existed even between $3d$ ions separated by one negative ion. Anderson (1959) considered a molecular orbitals formed of the admixture of the localized $3d$ orbitals and p orbitals of the intervening negative ion. The bonding orbital is mainly occupied by a negative ion, while the antibonding orbital is partially occupied by $3d$ electrons, leading to the magnetism of the system. Thus the wavefunction of localized d spins extends over the neighboring negative ion. There is a probability of transferring from one $3d$ orbital of the magnetic ion to the neighboring $3d$ orbitals, leading to the exchange interaction.

A considerably more satisfactory system of semi-empirical rules was developed over a period of years mainly by Goodenough and Kanamori. These rules have the important features of taking into account the occupation of the various d levels as dictated by ligand field theory. They are related to the prescriptions of Anderson's paper about the sign of superexchange. The main features of the superexchange interactions are usually explained in terms of the so-called Goodenough-Kanamori-Anderson rules. According to these rules, a 180° superexchange (the magnetic ion-ligand-magnetic ion angle is 180°) of two magnetic ions with partially filled d shells is strongly antiferromagnetic, whereas a 90° superexchange interaction is ferromagnetic and much weaker.

Content

1. Introduction
2. Direct exchange interaction
 - 2.1 Heitler-London model
 - 2.2 Direct exchange interaction in the case of the zero overlap integral
 - 2.3 Dirac spin-exchange operator
 - 2.4 Clebsch-Gordan co-efficient
 - A. Addition of two spin $S (=1/2)$
 - B. Mathematica program for the Clebsch-Gordan coefficient
3. Exchange interaction due to the electron transfer
 - 3.1 Localized spins and itinerant spins
 - 3.2 Hubbard model
 - 3.3 Eigenvalue problem
 - 3.4 Effective spin Hamiltonian for Mott insulator
 - 3.5 Mathematica program: eigenvalue problem for the Hubbard model
4. Superexchange interaction (first approach by Anderson 1950)
5. Superexchange interaction (revised approach by Anderson 1959)
 - 5.1 Molecular orbital due to d - p mixing
 - 5.2 Slater wavefunctions due to the d - p orbital mixing.
 - 5.3 Evaluation of superexchange interaction
 - 5.4 Simple model of p - d mixing
 - A. Eigenvalue problem
 - B. Perturbation approach
 - C. Mathematica program for the case A
6. Molecular orbitals
 - 6.1 hybridization of $2s$ and $2p(z)$ orbitals
 - 6.2 Mixing of $d\gamma$ - p_σ and $d\gamma$ - p_π orbitals
 - A. Antibonding molecular orbital of $d(3z^2-r^2)$ and $p(z) (=p_\sigma)$
 - A. Antibonding molecular orbital of $d(3z^2-r^2)$ and $p(x) (=p_\pi)$
 - 6.3. Mixing of $d\varepsilon$ - p_σ and $d\varepsilon$ - p_π orbitals
 - A. Antibonding molecular orbital of $d(zx)$ and $p(z) (=p_\sigma)$
 - B. Antibonding molecular orbital of $d(zx)$ and $p(x) (=p_\pi)$
7. Goodenough-Kanamori-Anderson (GKA) rules
 - 7.1 Definition of 180° and 90° superexchange interactions
 - 7.2 General rules for GKA (by Anderson)
 - 7.3. GKA rules for the 180° interaction \perp
 - A. $d\varepsilon \perp p_\sigma$
 - B. $d\gamma \not\perp p_\sigma$
 - C. $d\gamma \perp p_\pi$
 - D. $d\varepsilon \not\perp p_\pi$
 - 7.4. GKA rules for the 90° interaction
8. Application of GKA rules to real systems
 - 8.1 180° configuration
 - A. CaMnO_3 180° case; $(3d)^5$
 - B. NiO 180° case; $(3d)^8$
 - C. LaFeO_3 , MnO 180° case

- D. $\text{Ni}^{2+} (3d)^8$ and $\text{V}^{2+} (3d)^3$ 180° case
- E. $\text{Fe}^{3+} (3d)^5$ and $\text{Cr}^{3+} (3d)^3$ 180° case
- 8.2 90° configuration
 - A. NiCl_2
 - B. CoCl_2
 - C. CrCl_3
 - D. Ni^{2+} and V^{2+} 90° interaction
 - E. MnCl_2
 - F. CuCl_2
- 9. Application: La_2CuO_4 as a Mott insulator
- 10. Conclusion
- References
- Appendix
 - A. Mathematica program
 - B. Magnetic properties of typical magnetic compounds

((Note))

In this note we use the following notations for the $3d$ orbitals. $d\varepsilon = t_{2g} = d(xy)$, $d(yz)$, and $d(zx)$. $d\gamma = e_g = d(x^2 - y^2)$ and $d(3z^2 - r^2)$.

1. Introduction

The magnetism of the matters is an essentially quantum phenomenon. In 1928 Heisenberg¹ proposed a theory of ferromagnetism, based on the quantum mechanics. In the ferromagnets such as Fe, Co, and Ni, atoms or ions forming the matters have localized d electrons. He considered that there is a ferromagnetic exchange interaction ($J > 0$), in the form of

$$-2JS_i \cdot S_j. \quad (1.1)$$

When two wavefunctions are orthogonal, this interaction leads to a ferromagnetic spin order where all the spins of ions are aligned along the same direction. In other words, there are two kinds of interactions between two electrons; repulsive Coulomb interaction and a exchange interaction. The exchange interaction occurs as a result of the Pauli exclusion principle in the quantum mechanics. It is responsible for the Weiss molecular field generated in ferromagnets. This form of the exchange interaction is called a Heisenberg model for the magnetism of localized spins. (See Sec.2.2 for the detail.)

The importance of the exchange interaction received attention before Heisenberg proposed his theory. It was proposed by Heitler and London² that the interaction is the cause of covalent bonding of hydrogen molecules. In this case, there is an attractive Coulomb interaction between the electron of one atom and the nucleus of the other atom as well as a repulsive Coulomb interaction between two electrons. Thus the exchange integral J is negative and the ground state is a spin singlet, when the overlap integral between two wavefunctions are not equal to zero. (See Sec.2.1 for the detail.)

In 1949, Shull and Smart³ had carried out a neutron diffraction and demonstrated that MnO is an antiferromagnet. The nearest-neighbor Mn^{2+} ions are connected through an intervening O^{2-} . The interaction between Mn^{2+} ions is antiferromagnetic, and is called a superexchange interaction. Such interaction is rather different from the direct exchange interaction proposed by Heisenberg.¹

Originally superexchange acquired its name because of the relatively large distances, occupied by normally diamagnetic ions, radicals, or molecules. Small exchange coupling existed even between ions separated by one or several diamagnetic groups. The mechanism of superexchange was first introduced by Kramers⁴ (1934). He tried to explain the exchange interaction in paramagnetic salts. He pointed out that the ions could cause spin dependent perturbations in the wavefunctions of intervening ions, thereby transmitting the exchange effect over large distances, but no specific mechanism were discussed.

In 1950, Anderson⁵ refined the Kramers' approach. The idea can be illustrated by two Mn^{2+} and one O^{2-} ions arranged collinearly. The simplest model requires the consideration of four electrons. The ground state consists of one electron on each Mn^{2+} in the states d_1 and d_2 , and two electrons on the O^{2-} ion in identical p orbitals. The p orbitals have a dumbbell shape that coincides with the axis joining the two Mn^{2+} ions. Because of the overlap of their wavefunctions, one of p electrons from the O^{2-} ion hops over to one of the Mn^{2+} ions. The remaining unpaired p electron on O^{2-} ion then enters into a direct exchange with one d_2 electron of the other Mn^{2+} ion. The superexchange interaction between Mn^{2+} spins is then antiferromagnetic.

After further refinement, it was realized that this type of theory became involved in increasing uncertainties and complexities. In this theory the exchange effect appears in a third order of the perturbation theory. One encountered some difficulty. This perturbation theory is poorly convergent. The early terms which do not lead to magnetic effects are rather large.

In order to overcome such a difficulty, Anderson⁶ (1959) proposed a new theory of the superexchange interaction from a different view point. He considered molecular orbitals formed of the admixture of the localized $3d$ orbitals and p orbitals of the intervening negative ion. There are two orbitals thus obtained; the bonding orbital and the antibonding orbital. The bonding orbital is mainly occupied by a negative ion, while the antibonding orbital is partially occupied by $3d$ electrons, leading to the magnetism of the system. Thus the wavefunction of localized d spins extends over the neighboring negative ion. There is a probability of transferring from one $3d$ orbital of the magnetic ion to the neighboring $3d$ orbitals. The repulsive Coulomb interaction tends to prevent such a transition. In other words, when one d electron of the magnetic ions jumps into the unoccupied site of the neighboring magnetic ions, there is an energy increase by U , where U is the repulsive Coulomb interaction. In this picture, the first-order of the perturbation is a usual ferromagnetic exchange interaction, while the second-order of the perturbation is an antiferromagnetic exchange interaction and is expressed by

$$4 \frac{t^2}{U} \mathbf{S}_1 \cdot \mathbf{S}_2, \quad (1.2)$$

where t is the transition matrix of the transition of the electron in one atom to the neighboring atom and U is the Coulomb interaction between two electrons with different spin directions in the same atom. This is a new approach of the superexchange interaction by Anderson.⁶ This Hamiltonian is called as a Hubbard Hamiltonian. In the limit of $U \ll t$, electron can move around in the crystal, forming conduction electrons in the metal. In contrast, in the limit of $U \gg t$, electrons are localized in the lattice point, forming the insulator. The superexchange interaction results from a perturbation energy

from the insulator as a limiting case. It is concluded from the above discussion that the exchange interaction can be expressed by the general form

$$-2J_{12}\mathbf{S}_1 \cdot \mathbf{S}_2, \quad (1.3)$$

for both the direct exchange interaction and the superexchange interaction. Nevertheless, we encounter a difficulty in evaluating the magnitude and sign of J_{12} from the first principle of the quantum mechanics. (See Sec. 3 – 6 for the detail.)

A considerably more satisfactory system of semi-empirical rules was developed over a period of years by Goodenough⁷ and Kanamori.⁸ These rules have the important features of taking into account the occupation of the various d levels as dictated by ligand field theory. They are related to the prescriptions of Anderson's paper⁶ about the sign of superexchange. The exchange interaction in magnetic insulators is predominantly caused by the so-called superexchange – which is due to the overlap of the localized orbitals of the magnetic electrons with those of intermediate ligands. The main features of the superexchange interactions are usually explained in terms of the so-called Goodenough-Kanamori-Anderson rules.^{8,9,10} According to these rules, a 180° superexchange (the magnetic ion-ligand-magnetic ion angle is 180°) of two magnetic ions with partially filled d shells is strongly antiferromagnetic, whereas a 90° superexchange interaction is ferromagnetic and much weaker. (See Sec. 7 and 8).

2. Direct exchange interaction

2.1 Heitler-London model

We consider a hydrogen molecule (two-electron system). The two proton atoms are located at \mathbf{r}_a and \mathbf{r}_b . This was first considered by Heitler and London² in 1927. In the limit of infinite separation we assume that we have two neutral hydrogen atoms, where there is one electron around each proton. The Hamiltonian is given by

$$H = -\frac{\hbar^2}{2m}\nabla_1^2 - \frac{\hbar^2}{2m}\nabla_2^2 - \frac{e^2}{|\mathbf{r}_1 - \mathbf{r}_a|} - \frac{e^2}{|\mathbf{r}_2 - \mathbf{r}_b|} - \frac{e^2}{|\mathbf{r}_2 - \mathbf{r}_a|} - \frac{e^2}{|\mathbf{r}_1 - \mathbf{r}_b|} + \frac{e^2}{|\mathbf{r}_1 - \mathbf{r}_2|} + \frac{e^2}{|\mathbf{r}_a - \mathbf{r}_b|}, \quad (2.1)$$

where m is a mass of electron. When the distance between two hydrogens are sufficiently long, they are regarded as isolated hydrogen atoms. The Schrödinger equation of each hydrogen atom is given by

$$\begin{aligned} \left(-\frac{\hbar^2}{2m}\nabla_1^2 - \frac{e^2}{|\mathbf{r}_1 - \mathbf{r}_a|}\right)\phi_a(\mathbf{r}_1) &= E_0\phi_a(\mathbf{r}_1) \\ \left(-\frac{\hbar^2}{2m}\nabla_2^2 - \frac{e^2}{|\mathbf{r}_2 - \mathbf{r}_b|}\right)\phi_b(\mathbf{r}_2) &= E_0\phi_b(\mathbf{r}_2) \end{aligned}, \quad (2.2)$$

where E_0 is the energy eigenvalue, and $\langle \mathbf{r}_1 | \phi_a \rangle = \phi_a(\mathbf{r}_1)$ and $\langle \mathbf{r}_2 | \phi_b \rangle = \phi_b(\mathbf{r}_2)$ are the energy eigenfunction.

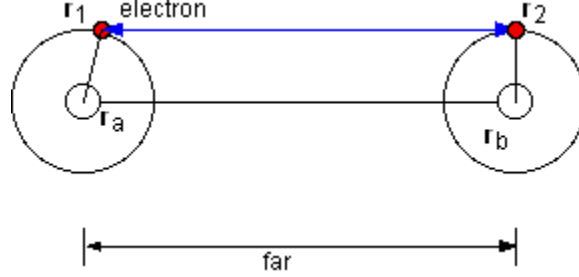


Fig.1 Model of hydrogen molecule. Protons at r_a and r_b . Electrons at r_1 and r_2 .

Since

$$[\hat{P}_{12}, \hat{H}] = 0, \quad (2.3)$$

we have a simultaneous eigenket of \hat{P}_{12} and \hat{H} :

$$\hat{H}|\psi\rangle = E|\psi\rangle \text{ and } \hat{P}_{12}|\psi\rangle = \lambda|\psi\rangle. \quad (2.4)$$

Since $\hat{P}_{12}^2 = 1$,

$$\hat{P}_{12}^2|\psi\rangle = \lambda\hat{P}_{12}|\psi\rangle = \lambda^2|\psi\rangle = |\psi\rangle, \quad (2.5)$$

we have $\lambda = \pm 1$. Since the spins are fermion, the wave function should be antisymmetric under the exchange of two particles.

Here we discuss the eigenvalue and eigenfunction of the system.¹¹ The Hamiltonian \hat{H} of the system in the case of no magnetic field does not contain the spin operators, and hence, when it is applied to the wave function, it has no effect on the spin variables. The wave function of the system of particles can be written in the form of product,

$$|\psi\rangle = |\psi_{space}\rangle |\chi_{spin}\rangle, \quad (2.6)$$

where $|\psi_{space}\rangle$ depends only on the co-ordinates of the particles and $|\chi_{spin}\rangle$ only on their spins. If the Hamiltonian \hat{H} contains the spin operators, the separation of the spacial part and spin part is not possible. We need to introduce the Slater determinant. For the two particle systems, the wavefunction can be described by

$$|\psi\rangle = \frac{1}{\sqrt{N}} \begin{vmatrix} |\phi_a\rangle_1 |\alpha\rangle_1 & |\phi_a\rangle_2 |\alpha\rangle_2 \\ |\phi_b\rangle_1 |\beta\rangle_1 & |\phi_b\rangle_2 |\beta\rangle_2 \end{vmatrix}, \quad (2.7)$$

where N is the normalization factor, $|\phi_i\rangle$ ($i = a, b$) are the spatial states of the isolated hydrogen atom, $|\alpha\rangle, |\beta\rangle$ are the spin states, the index 1 and 2, are the positions of particles.

If the Hamiltonian \hat{H} does not contain the spin operators, the spacial wavefunction can be described by the antisymmetric wavefunction (Baym¹²)

$$|\psi_{space}^a\rangle = \frac{1}{\sqrt{2(1-\ell^2)}} \begin{vmatrix} |\phi_a\rangle_1 & |\phi_a\rangle_2 \\ |\phi_b\rangle_1 & |\phi_b\rangle_2 \end{vmatrix}, \quad (2.8)$$

for the triplet spin state ($S = 1$) and by the symmetric wave function

$$|\psi_{space}^s\rangle = \frac{1}{\sqrt{2(1+\ell^2)}} [|\phi_a\rangle_1 |\phi_b\rangle_2 + |\phi_b\rangle_1 |\phi_a\rangle_2], \quad (2.9)$$

for the singlet spin state ($S = 0$), where ℓ is the overlap integral, $\langle \phi_a | \phi_b \rangle = \ell$. The singlet spin state is expressed by $|\chi_{spin}\rangle = \frac{1}{\sqrt{2}}[|+-\rangle - |-+\rangle]$ (see Sec. 2.4A).

The expectation value of the Hamiltonian in the states $|\psi_{space}^s\rangle$ and $|\psi_{space}^a\rangle$ is

$$E_{\pm} = \langle H \rangle_{\pm} = \frac{\langle ab|H|ab\rangle + \langle ba|H|ba\rangle \pm \langle ab|H|ba\rangle \pm \langle ba|H|ab\rangle}{2 \pm 2\ell^2}, \quad (2.10)$$

where the upper sign denotes the singlet spin state, the lower the triplet, and

$$\begin{aligned} \langle ab|H|ab\rangle &= \int d\mathbf{r}_1 \int d\mathbf{r}_2 \langle \mathbf{r}_1 | \phi_a \rangle^* \langle \mathbf{r}_2 | \phi_b \rangle^* H \langle \mathbf{r}_1 | \phi_a \rangle \langle \mathbf{r}_2 | \phi_b \rangle \\ \langle ba|H|ba\rangle &= \int d\mathbf{r}_1 \int d\mathbf{r}_2 \langle \mathbf{r}_1 | \phi_b \rangle^* \langle \mathbf{r}_2 | \phi_a \rangle^* H \langle \mathbf{r}_1 | \phi_b \rangle \langle \mathbf{r}_2 | \phi_a \rangle \\ \langle ab|H|ba\rangle &= \int d\mathbf{r}_1 \int d\mathbf{r}_2 \langle \mathbf{r}_1 | \phi_a \rangle^* \langle \mathbf{r}_2 | \phi_b \rangle^* H \langle \mathbf{r}_1 | \phi_b \rangle \langle \mathbf{r}_2 | \phi_a \rangle \\ \langle ba|H|ab\rangle &= \int d\mathbf{r}_1 \int d\mathbf{r}_2 \langle \mathbf{r}_1 | \phi_b \rangle^* \langle \mathbf{r}_2 | \phi_a \rangle^* H \langle \mathbf{r}_1 | \phi_a \rangle \langle \mathbf{r}_2 | \phi_b \rangle \end{aligned} \quad (2.11)$$

Because of $\langle ba|H|ba\rangle = \langle ab|H|ab\rangle$ and $\langle ab|H|ba\rangle = \langle ba|H|ab\rangle$, we have

$$E_{\pm} = \langle H \rangle_{\pm} = \frac{\langle ab|H|ab\rangle \pm \langle ba|H|ab\rangle}{1 \pm \ell^2}, \quad (2.12)$$

where

$$\langle ab|H|ab\rangle = 2E_0 + \frac{e^2}{R_{ab}} + V_c, \quad (2.13)$$

$$\langle ba|H|ab\rangle = \ell^2(2E_0 + \frac{e^2}{R_{ab}}) + V_{ex}. \quad (2.14)$$

Here $R_{ab} = |\mathbf{r}_a - \mathbf{r}_b|$, V_c is the Coulomb integral, and V_{ex} is the exchange contribution to the electron energy

$$\begin{aligned} V_c &= \int d\mathbf{r}_1 \int d\mathbf{r}_2 |\langle \mathbf{r}_1 | \phi_a \rangle|^2 |\langle \mathbf{r}_2 | \phi_b \rangle|^2 \left[-\frac{e^2}{|\mathbf{r}_2 - \mathbf{r}_a|} - \frac{e^2}{|\mathbf{r}_1 - \mathbf{r}_b|} + \frac{e^2}{|\mathbf{r}_1 - \mathbf{r}_2|} \right] \\ V_{ex} &= \int d\mathbf{r}_1 \int d\mathbf{r}_2 \langle \mathbf{r}_1 | \phi_a \rangle^* \langle \mathbf{r}_2 | \phi_b \rangle^* \langle \mathbf{r}_1 | \phi_b \rangle \langle \mathbf{r}_2 | \phi_a \rangle \left[-\frac{e^2}{|\mathbf{r}_2 - \mathbf{r}_a|} - \frac{e^2}{|\mathbf{r}_1 - \mathbf{r}_b|} + \frac{e^2}{|\mathbf{r}_1 - \mathbf{r}_2|} \right] \end{aligned} \quad (2.15)$$

Then we have

$$E_{\pm} = 2E_0 + \frac{e^2}{R_{ab}} + \frac{V_c \pm V_{ex}}{1 \pm \ell^2}, \quad (2.16)$$

or

$$E_{\pm} = 2E_0 + \frac{(V_c + \frac{e^2}{R_{ab}}) \pm (V_{ex} + \ell^2 \frac{e^2}{R_{ab}})}{1 \pm \ell^2}. \quad (2.17)$$

The term $V_c + \frac{e^2}{R_{ab}}$ is always positive, while $V_{ex} + \ell^2 \frac{e^2}{R_{ab}}$ is in general negative. Thus E_+ (singlet spin state) is lower than E_- (triplet spin state). So we can conclude that the H_2

molecule binds in the spin singlet state, but not in the triplet state. The strength of the binding is roughly proportional to the amount of the overlap of the two electron states.

((Note))

In the Heitler-London model, the overlap integral ℓ is not equal to zero since $|\phi_a\rangle = |1s\rangle$ and $|\phi_b\rangle = |1s\rangle$. In this case, V_{ex} becomes negative, favoring the singlet spin state ($S = 0$) or antiferromagnetic spin alignment.

2.2 Direct exchange interaction in the case of the zero overlap integral

We now consider the simple case when the overlap integral is equal to zero; $\langle\phi_a|\phi_b\rangle = \ell = 0$ (orthogonal). The electron energy is given by

$$E_{\pm} = 2E_0 + \frac{e^2}{R_{ab}} + V_c \pm V_{ex} = 2E_0 + \frac{e^2}{R_{ab}} + K \pm J, \quad (2.18)$$

where

$$\begin{aligned} V_{ex} = J &= \int d\mathbf{r}_1 \int d\mathbf{r}_2 \langle \mathbf{r}_1 | \phi_a \rangle^* \langle \mathbf{r}_2 | \phi_b \rangle^* \frac{e^2}{|\mathbf{r}_1 - \mathbf{r}_2|} \langle \mathbf{r}_1 | \phi_b \rangle \langle \mathbf{r}_2 | \phi_a \rangle \\ V_c = K &= \int d\mathbf{r}_1 \int d\mathbf{r}_2 \langle \mathbf{r}_1 | \phi_a \rangle^2 \langle \mathbf{r}_2 | \phi_b \rangle^2 \left[-\frac{e^2}{|\mathbf{r}_2 - \mathbf{r}_a|} - \frac{e^2}{|\mathbf{r}_1 - \mathbf{r}_b|} + \frac{e^2}{|\mathbf{r}_1 - \mathbf{r}_2|} \right]. \end{aligned} \quad (2.19)$$

The matrix of \hat{H} in the basis of $|\psi_{space}^{(s)}\rangle$ and $|\psi_{space}^{(a)}\rangle$ is calculated as

$$\begin{aligned} \langle \psi_{space}^{(s)} | \hat{H} | \psi_{space}^{(s)} \rangle &= K + J \\ \langle \psi_{space}^{(a)} | \hat{H} | \psi_{space}^{(a)} \rangle &= K - J, \end{aligned} \quad (2.20)$$

or

$$\begin{aligned} \hat{H} | \psi_{space}^{(s)} \rangle &= (K + J) | \psi_{space}^{(s)} \rangle \\ \hat{H} | \psi_{space}^{(a)} \rangle &= (K - J) | \psi_{space}^{(a)} \rangle. \end{aligned} \quad (2.21)$$

The integral K is called as the Coulomb integral. The integral J is called an exchange integral. Here we can prove that J is always positive. The Fourier transform of the Coulomb interaction is given by

$$\frac{e^2}{r_{12}} = \frac{1}{\Omega} \sum_{\mathbf{q}} \frac{4\pi e^2}{q^2} e^{i\mathbf{q} \cdot (\mathbf{r}_1 - \mathbf{r}_2)}. \quad (2.22)$$

The substitution of this into the integral J leads to

$$\begin{aligned} J &= \frac{4\pi e^2}{\Omega} \sum_{\mathbf{q}} \frac{1}{q^2} \int d^3 r_1 \langle \mathbf{r}_1 | \phi_a \rangle^* \langle \mathbf{r}_1 | \phi_b \rangle e^{i\mathbf{q} \cdot \mathbf{r}_1} \int d^3 r_2 \langle \mathbf{r}_2 | \phi_b \rangle^* \langle \mathbf{r}_2 | \phi_a \rangle e^{-i\mathbf{q} \cdot \mathbf{r}_2} \\ &= \frac{4\pi e^2}{\Omega} \sum_{\mathbf{q}} \frac{1}{q^2} \left| \int d^3 r_1 \langle \mathbf{r}_1 | \phi_a \rangle^* \langle \mathbf{r}_1 | \phi_b \rangle e^{i\mathbf{q} \cdot \mathbf{r}_1} \right|^2 > 0. \end{aligned} \quad (2.23)$$

We note that the spin part $|\chi_{spin}\rangle$ is symmetric ($S = 1$, triplet) for $|\psi_{space}^{(a)}\rangle$ and antisymmetric ($S = 0$, singlet) for $|\psi_{space}^{(s)}\rangle$, respectively. Since $J > 0$, the energy of the spin triplet state ($= K - J$) is lower than that of the spin singlet state ($= K + J$). In other words, the ferromagnetic spin alignment is energetically favorable (Heisenberg model).

In general, the direct exchange is ferromagnetic if the two orbitals $|\varphi_a\rangle$ and $|\varphi_b\rangle$ are orthogonal. If two orbitals $|\varphi_a\rangle$ and $|\varphi_b\rangle$ are not orthogonal, then the magnitude of the overlap integral provide a measure for the covalency of these orbitals. This rule will be used in Sec.7.

2.3 Dirac spin-exchange operator

We use the Dirac exchange operator¹¹:

$$\hat{P}_{12} = \frac{1}{2}(1 + \hat{\sigma}_1 \cdot \hat{\sigma}_2) = \frac{1}{2}(1 + 4\hat{S}_1 \cdot \hat{S}_2) = \frac{1}{2} + 2\hat{S}_1 \cdot \hat{S}_2. \quad (2.24)$$

Since $S_1 = \frac{1}{2}\sigma_1$ and $S_2 = \frac{1}{2}\sigma_2$

$$\hat{P}_{12}|\chi_{\text{singlet}}\rangle = \left(\frac{1}{2} + 2\hat{S}_1 \cdot \hat{S}_2\right)|\chi_{\text{singlet}}\rangle = -|\chi_{\text{singlet}}\rangle \quad (\text{antisymmetric}), \quad (2.25)$$

$$\hat{P}_{12}|\chi_{\text{triplet}}\rangle = \left(\frac{1}{2} + 2\hat{S}_1 \cdot \hat{S}_2\right)|\chi_{\text{triplet}}\rangle = |\chi_{\text{triplet}}\rangle \quad (\text{symmetric}) \quad (2.26)$$

or

$$\hat{S}_1 \cdot \hat{S}_2|\chi_{\text{singlet}}\rangle = -\frac{3}{4}|\chi_{\text{singlet}}\rangle, \quad (2.27)$$

$$\hat{S}_1 \cdot \hat{S}_2|\chi_{\text{triplet}}\rangle = \frac{1}{4}|\chi_{\text{triplet}}\rangle. \quad (2.28)$$

We define the Spin Hamiltonian (exchange energy) by

$$\hat{H}_s = K - 2J(\hat{S}_1 \cdot \hat{S}_2 + \frac{1}{4}). \quad (2.29)$$

Since J is positive, the interaction is ferromagnetic.

$$\hat{H}_s|\chi_{\text{singlet}}\rangle = [K - J(\frac{1}{2} + 2\hat{S}_1 \cdot \hat{S}_2)]|\chi_{\text{singlet}}\rangle = (K + J)|\chi_{\text{singlet}}\rangle, \quad (2.30)$$

$$\hat{H}_s|\chi_{\text{triplet}}\rangle = [K - J(\frac{1}{2} + \frac{2}{\hbar^2}\hat{S}_1 \cdot \hat{S}_2)]|\chi_{\text{triplet}}\rangle = (K - J)|\chi_{\text{triplet}}\rangle. \quad (2.31)$$

The above equation is usually referred to as the Heisenberg exchange interaction.

2.4 Clebsch-Gordan co-efficient

A Addition of two spin $S (=1/2)$

The results of the calculation are summarized as follows (Sakurai¹¹)

$$j_1 = 1/2, j_2 = 1/2 \quad (|m_1| \leq 1/2, |m_2| \leq 1/2)$$

$$D_{1/2} \times D_{1/2} = D_1 + D_0$$

(i) $j = 1$ (symmetric)

$$m = m_1 + m_2$$

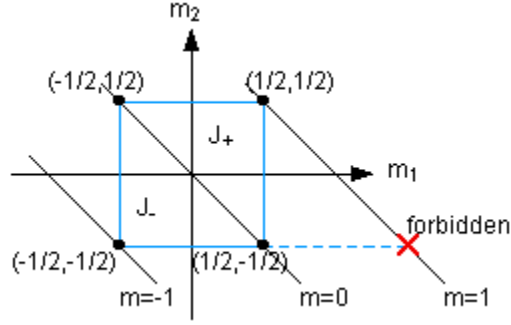


Fig.2 Recursion relations to obtain the Clebsch-Gordon co-efficients for $|j, m\rangle$, where $j = 1$ and $m = 1, 0$, and -1 .

$$\left| j_1 = \frac{1}{2}, m_1 = \frac{1}{2} \right\rangle \left| j_2 = \frac{1}{2}, m_2 = \frac{1}{2} \right\rangle \quad (m = 1), \quad (2.32)$$

$$\frac{\left| \frac{1}{2}, \frac{1}{2} \right\rangle \left| \frac{1}{2}, -\frac{1}{2} \right\rangle + \left| \frac{1}{2}, -\frac{1}{2} \right\rangle \left| \frac{1}{2}, \frac{1}{2} \right\rangle}{\sqrt{2}} \quad (m = 0), \quad (2.33)$$

$$\left| \frac{1}{2}, -\frac{1}{2} \right\rangle \left| \frac{1}{2}, -\frac{1}{2} \right\rangle \quad (m = -1). \quad (2.34)$$

(ii) $j = 0$ ($m = 0$) (antisymmetric)

$$\frac{\left| \frac{1}{2}, \frac{1}{2} \right\rangle \left| \frac{1}{2}, -\frac{1}{2} \right\rangle - \left| \frac{1}{2}, -\frac{1}{2} \right\rangle \left| \frac{1}{2}, \frac{1}{2} \right\rangle}{\sqrt{2}} \quad (m = 0). \quad (2.35)$$

B. Mathematica program for the Clebsch-Gordan coefficient

Determination of CG co-efficient

Addition of $S_1=1/2, S_2=1/2$

```
CG[j1_, j2_, j_] := Table[Sum[ClebschGordan[{j1, k1}, {j2, k2}, {j, k1+k2}] a[j1, k1] b[j2, k2] KroneckerDelta[k1+k2, m], {k1, -j1, j1}, {k2, -j2, j2}], {m, -j, j}]
CG[1/2, 1/2, 1] // TableForm
a[1/2, -1/2] b[1/2, -1/2]
a[1/2, 1/2] b[1/2, -1/2] + a[1/2, -1/2] b[1/2, 1/2]
a[1/2, 1/2] b[1/2, 1/2]
CG[1/2, 1/2, 0] // TableForm
a[1/2, 1/2] b[1/2, -1/2] - a[1/2, -1/2] b[1/2, 1/2]
```

3. Exchange interaction due to the electron transfer

3.1 Localized spins and itinerant spins

In the ferromagnetic theory proposed by Heisenberg,¹ it is assumed that the $3d$ electrons are localized around atoms. Since the orbital angular momentum is almost quenched, we consider only the spin angular momentum. According to the Hund's law, the spin S is given by $S = 2$ for $(3d)^6$ (Fe^{2+}) and $S = 3/2$ for $(3d)^7$. Correspondingly, the spin magnetic moment is $4\mu_B$ per atom for $(3d)^6$ and $3\mu_B$ per atom for $(3d)^7$, respectively. The measurement of the saturation magnetization at low temperatures shows that the magnetic moment is $2.22 \mu_B$, corresponding to the electron configuration $(3d)^{7.78}$. This implies that the $3d$ electrons are not localized, but rather itinerant. Anderson⁶ have shown that in magnetic insulator compounds the d electrons are localized owing to the Mott mechanism of strong correlation. Relatively weak covalency between localized states or delocalization mechanism gives rise to the superexchange interaction of usually antiferromagnetic sign between the local moments.

The localized model starts with the electronic states localized in the real space, while the itinerant model starts with those localized in the reciprocal or wave-vector space. What happens to the interactions between the d electrons when the d electrons are itinerant? In order to understand the essential point for the difference between these model, here we now consider a solid formed of hydrogen atoms (see Fig.1). The separation distance is d . Each hydrogen atom has one electron in average. We assume that the orbital state of each atom is in the $1s$ state. When the lattice constant d becomes shorter, the energy band is formed. Since there is one (odd number) electron per unit cell, it is predicted from the energy band theory that the system should be a metal with a half-filled band. Here we assume a repulsive Coulomb interaction U between electrons with different spin states ($|\uparrow\rangle$ and $|\downarrow\rangle$) in the same atom, and the transition matrix t for electrons to jump from one atom to the nearest neighbor atoms. The state of the atom is characterized by the number of electrons; neutral state (the number of electrons is 1), and ionic states (the number of electrons is 0 or 2). When U is much larger than t , the electron transfer does not occur at all. It is expected that a state close to the isolated ionic is realized (Mott insulator^{13,14}). On the other hand, when t is much larger than U , the electrons move about the whole crystal and behave as conduction electrons. The difference between these two cases is controlled by the relative magnitude of t and U in the Hamiltonian. When the ratio of t to U is changed, a transition is expected to occur from one state to the other state. This transition (which is presumably discontinuous in three and two dimensions) is called the Mott transition or the Mott problem in the electron theory of solids. The Hamiltonian is called the Hubbard Hamiltonian, although it was used before the work of Hubbard.

3.2 Hubbard model

The Hubbard Hamiltonian has been proposed to discuss the electron correlation in the spin system. In this model, the correlation on the same atom is considered to be important.

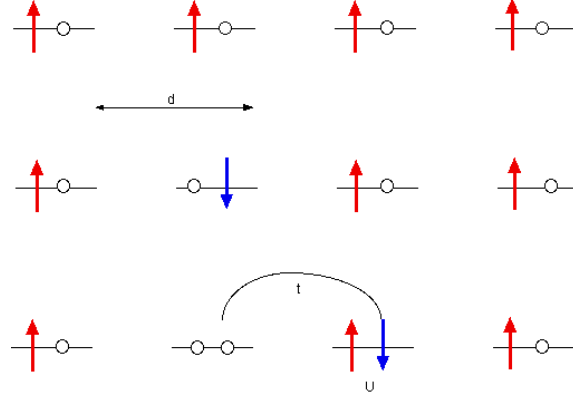


Fig.3 One-dimensional model of hydrogen-atom solid, where the lattice constant is d . Each atom has one of four states $|\uparrow, \downarrow\rangle$, $|\uparrow, 0\rangle$, $|0, \downarrow\rangle$, and $|0, 0\rangle$, where $|0\rangle$ is an empty state. U is a repulsive Coulomb interaction between electrons with different spin states in the same atom. t is the transition matrix for electrons to jump from one atom to the nearest neighbor atoms.

We consider a simple model when each electron is in the (1s) state. There is one electron per atom. In each atom, there are two spin states: up-spin state and down-spin state. According to the Pauli's exclusive principle, there are four states in each atom; ionic state (one empty state, two one-electron states), and a neutral state (one two-electron state).

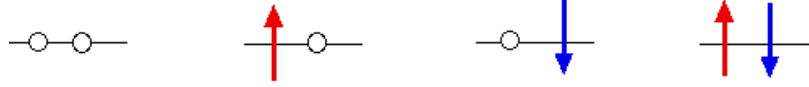


Fig.4 Each atom has one of four states $|\uparrow, \downarrow\rangle$, $|\uparrow, 0\rangle$, $|0, \downarrow\rangle$, and $|0, 0\rangle$, where $|0\rangle$ is an empty state.

We assume that the distance between atoms is constant (d). When d is small, the system becomes metal with half-filled band. In an ionic state where two electrons are occupied in the up-spin state and the down-spin state, the repulsive Coulomb energy between two electrons leads to the increase of energy of the system. When d becomes large, the probability of jumping from one atom to the adjacent atom becomes small.

We assume that t_{ij} is the transfer integral between the sites i and j (denoted by \mathbf{R}_i and \mathbf{R}_j). U is the Coulomb interaction between two electrons in the same atom. The model Hamiltonian H is given by a so-called Hubbard model (Yosida,¹⁵ Shiba¹⁶)

$$H = \sum_{(i,j)\sigma} (t_{ij} c_{i\sigma}^+ c_{j\sigma} + h.c.) + U \sum_j n_{j\uparrow} n_{j\downarrow}, \quad (3.1)$$

where the summation is taken over the pair (i, j) , $c_{j\sigma}^+$ and $c_{j\sigma}$ are the creation and annihilation operators of electron with spin σ on the atom j . The number operator is defined by $n_{j\sigma} = c_{j\sigma}^+ c_{j\sigma}$. The commutation relations for these operators are given by

$$\begin{aligned}
\{c_{i\sigma}^+, c_{j\sigma'}^+\}_+ &= c_{i\sigma}^+ c_{j\sigma'}^+ + c_{j\sigma'} c_{i\sigma}^+ = \delta_{ij} \delta_{\sigma\sigma'}, \\
\{c_{i\sigma}, c_{j\sigma'}^+\}_+ &= 0 \\
\{c_{i\sigma}^+, c_{j\sigma'}^+\}_+ &= 0
\end{aligned} \tag{3.2}$$

The first term of the Hamiltonian is the translation term from the j -site to the i -site. The second term is the Coulomb interaction between the electrons with the up-state and down-spin state on the same atom and is the origin of electron correlation.

For simplicity we consider the system with only two atoms at the sites 1 and 2. There are two spin states (up-state and down-state) on the same atom. The relevant Hamiltonian is given by

$$H = t(c_{1\uparrow}^+ c_{2\uparrow} - c_{1\uparrow} c_{2\uparrow}^+ + c_{1\downarrow}^+ c_{2\downarrow} - c_{1\downarrow} c_{2\downarrow}^+) + U(n_{1\uparrow} n_{1\downarrow} + n_{2\uparrow} n_{2\downarrow}). \tag{3.3}$$

There are possible six states; $|\phi_1\rangle = |1\uparrow, 2\uparrow\rangle$, $|\phi_2\rangle = |1\uparrow, 2\downarrow\rangle$, $|\phi_3\rangle = |1\downarrow, 2\uparrow\rangle$, $|\phi_4\rangle = |1\uparrow, 1\downarrow\rangle$, $|\phi_5\rangle = |2\uparrow, 2\downarrow\rangle$, and $|\phi_6\rangle = |1\downarrow, 2\downarrow\rangle$. Note that there are two electrons at the same atoms for the states $|\phi_4\rangle$ and $|\phi_5\rangle$, while the atoms 1 and 2 are occupied by one electron for $|\phi_1\rangle$, $|\phi_2\rangle$, $|\phi_3\rangle$, and $|\phi_6\rangle$.

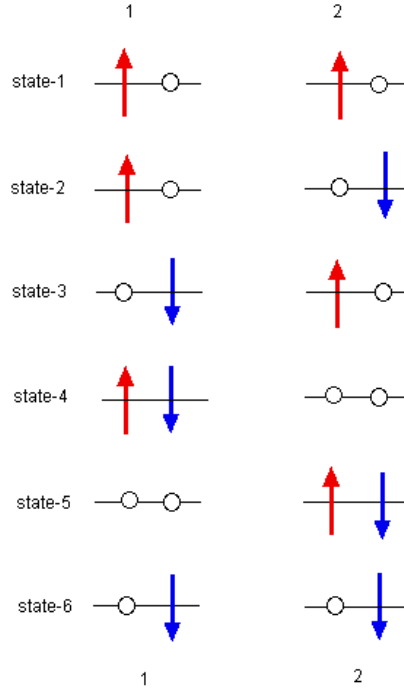


Fig.5 Possible states of two neighboring atoms located at positions (1) and (2).

The matrix element of the Hubbard Hamiltonian based on the above six states is given by

$$H = \begin{pmatrix} 0 & 0 & 0 & 0 & 0 & 0 \\ 0 & 0 & 0 & -t & -t & 0 \\ 0 & 0 & 0 & -t & -t & 0 \\ 0 & -t & -t & U & 0 & 0 \\ 0 & -t & -t & 0 & U & 0 \\ 0 & 0 & 0 & 0 & 0 & 0 \end{pmatrix}. \quad (3.4)$$

((Note))

$$\begin{aligned} H|\phi_4\rangle &= [t(c_{1\uparrow}^+ c_{2\uparrow} - c_{1\uparrow} c_{2\uparrow}^+ + c_{1\downarrow}^+ c_{2\downarrow} - c_{1\downarrow} c_{2\downarrow}^+) + U(n_{1\uparrow} n_{1\downarrow} + n_{2\uparrow} n_{2\downarrow})] |1\uparrow, 1\downarrow\rangle \\ &= -t |1\downarrow, 2\uparrow\rangle + U |1\uparrow, 1\downarrow\rangle - t |1\uparrow, 2\downarrow\rangle \\ &= -t |\phi_2\rangle - t |\phi_3\rangle + U |\phi_4\rangle \end{aligned} \quad (3.5)$$

3.3 Eigenvalue problem

We solve the eigenvalue problem using the Mathematica (sse below). The results are as follows. The energy eigenvalues and eigenkets

$$E = E_1 = 0, \quad |\psi_1\rangle = |\phi_6\rangle, \quad (3.6)$$

$$E = E_2 = 0, \quad |\psi_2\rangle = \frac{1}{\sqrt{2}}(|\phi_2\rangle - |\phi_3\rangle), \quad (3.7)$$

$$E = E_3 = 0, \quad |\psi_3\rangle = |\phi_1\rangle, \quad (3.8)$$

$$E = E_4 = U, \quad |\psi_4\rangle = \frac{1}{\sqrt{2}}(|\phi_4\rangle - |\phi_5\rangle), \quad (3.9)$$

$$\begin{aligned} E = E_5 &= \frac{1}{2}(U - \sqrt{U^2 + 16t^2}), \\ |\psi_5\rangle &= \frac{U + \sqrt{U^2 + 16t^2}}{4t}(|\phi_2\rangle + |\phi_3\rangle) + |\phi_4\rangle + |\phi_5\rangle, \end{aligned} \quad (3.10)$$

$$\begin{aligned} E = E_6 &= \frac{1}{2}(U + \sqrt{U^2 + 16t^2}) \\ |\psi_6\rangle &= \frac{U - \sqrt{U^2 + 16t^2}}{4t}(|\phi_2\rangle + |\phi_3\rangle) + |\phi_4\rangle + |\phi_5\rangle, \end{aligned} \quad (3.11)$$

where $|\psi_4\rangle$ and $|\psi_5\rangle$ are not normalized in order to avoid the complication. The ground state energy is E_5 and the corresponding eigenket is rewritten as

$$|\psi_5\rangle = \frac{U + \sqrt{U^2 + 16t^2}}{4t} \sqrt{2} \left(\frac{1}{\sqrt{2}} |\phi_2\rangle + \frac{1}{\sqrt{2}} |\phi_3\rangle \right) + \sqrt{2} \left(\frac{1}{\sqrt{2}} |\phi_4\rangle + \frac{1}{\sqrt{2}} |\phi_5\rangle \right). \quad (3.12)$$

Note that the eigenket $|\psi_5\rangle$ is rewritten as

$$|\psi_6\rangle = \frac{U - \sqrt{U^2 + 16t^2}}{4t} \sqrt{2} \left(\frac{1}{\sqrt{2}} |\phi_2\rangle + \frac{1}{\sqrt{2}} |\phi_3\rangle \right) + \sqrt{2} \left(\frac{1}{\sqrt{2}} |\phi_4\rangle + \frac{1}{\sqrt{2}} |\phi_5\rangle \right). \quad (3.13)$$

We now consider the two extreme cases.

(i) The case of $U \gg t$

$$E_1 = 0, E_2 = 0, E_3 = 0, E_4 = U, E_5 = -\frac{4t^2}{U}, \text{ and } E_6 = U + \frac{4t^2}{U}.$$

$$|\psi_5\rangle \approx \frac{U}{2t} \sqrt{2} \left(\frac{1}{\sqrt{2}} |\phi_2\rangle + \frac{1}{\sqrt{2}} |\phi_3\rangle \right) + \sqrt{2} \left(\frac{1}{\sqrt{2}} |\phi_4\rangle + \frac{1}{\sqrt{2}} |\phi_5\rangle \right), \quad (3.14)$$

or

$$|\psi_5\rangle \approx \frac{1}{\sqrt{2}} (|\phi_2\rangle + |\phi_3\rangle). \quad (3.15)$$

Note that this eigenket is normalized.

$$|\psi_6\rangle = \frac{1}{\sqrt{2}} (|\phi_4\rangle + |\phi_5\rangle). \quad (3.16)$$

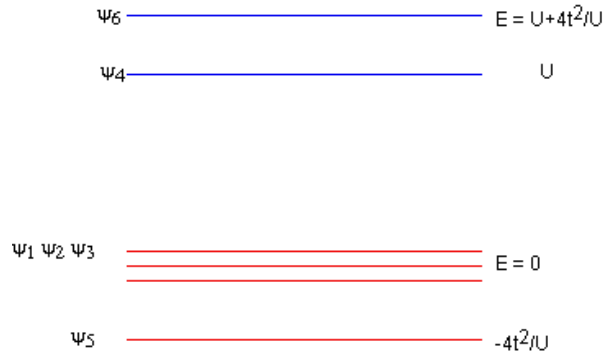


Fig.6 Energy levels of states $|\psi_i\rangle$ (i = 1 – 6).

$|\psi_1\rangle, |\psi_2\rangle, |\psi_3\rangle, |\psi_5\rangle$ are the states where atoms 1 and 2 are occupied by one electron.
 $|\psi_4\rangle, |\psi_6\rangle$ are the states where atom 1 (or atom 2) is occupied by two electrons.

$$\begin{aligned} |\psi_1\rangle &= |1 \uparrow, 2 \uparrow\rangle \\ |\psi_2\rangle &= \frac{1}{\sqrt{2}} (|1 \uparrow, 2 \downarrow\rangle - |1 \downarrow, 2 \uparrow\rangle) \\ |\psi_3\rangle &= |1 \downarrow, 2 \downarrow\rangle \\ |\psi_5\rangle &= \frac{1}{\sqrt{2}} (|1 \uparrow, 2 \downarrow\rangle + |1 \downarrow, 2 \uparrow\rangle) \\ H|\psi_5\rangle &= -\frac{4t^2}{U} |\psi_5\rangle. \end{aligned} \quad (3.17)$$

The addition of two electron spins of $S = 1/2$ gives the total spin $S = 1$ (symmetric state) and $S = 0$ (anti-symmetric state). $|\psi_1\rangle$ corresponds to $|S = 1, m = 1\rangle$. $|\psi_5\rangle$ corresponds to $|S = 1, m = 0\rangle$. $|\psi_3\rangle$ corresponds to $|S = 1, m = -1\rangle$. $|\psi_2\rangle$ corresponds to $|S = 0, m = 0\rangle$.

(ii) The case of $U \ll t$

$$E_1 = 0, E_2 = 0, E_3 = 0, E_4 = U, E_5 = \frac{1}{2}U - 2t, \text{ and } E_6 = \frac{1}{2}U + 2t$$

$$|\psi_5\rangle = \frac{|\phi_2\rangle + |\phi_3\rangle + |\phi_4\rangle + |\phi_5\rangle}{2}, \quad (3.18)$$

$$|\psi_6\rangle = \frac{-(|\phi_2\rangle + |\phi_3\rangle) + (|\phi_4\rangle + |\phi_5\rangle)}{2}. \quad (3.19)$$

Note that $|\psi_5\rangle$ is the ground state, where both the up and spin electrons occupy.

3.4 Effective spin Hamiltonian for Mott insulator¹⁴

We now consider the case of $U \gg t$, where atoms 1 and 2 are occupied by one electron ($|\phi_1\rangle = |1\uparrow, 2\uparrow\rangle$, $|\phi_2\rangle = |1\uparrow, 2\downarrow\rangle$, $|\phi_3\rangle = |1\downarrow, 2\uparrow\rangle$, and $|\phi_6\rangle = |1\downarrow, 2\downarrow\rangle$). We use the perturbation theory. The excited state are $|\phi_4\rangle = |1\uparrow, 1\downarrow\rangle$ and $|\phi_5\rangle = |2\uparrow, 2\downarrow\rangle$, where the atom is occupied by two electrons. The Hamiltonian consists of unperturbed Hamiltonian H_0 and the perturbation Hamiltonian H_1 ,

$$H = H_0 + H_1$$

$$= U(n_{1\uparrow}n_{1\downarrow} + n_{2\uparrow}n_{2\downarrow}) + t(c_{1\uparrow}^+ c_{2\uparrow} - c_{1\uparrow} c_{2\uparrow}^+ + c_{1\downarrow}^+ c_{2\downarrow} - c_{1\downarrow} c_{2\downarrow}^+), \quad (3.20)$$

where

$$H_0 = U(n_{1\uparrow}n_{1\downarrow} + n_{2\uparrow}n_{2\downarrow}),$$

$$H_1 = t(c_{1\uparrow}^+ c_{2\uparrow} - c_{1\uparrow} c_{2\uparrow}^+ + c_{1\downarrow}^+ c_{2\downarrow} - c_{1\downarrow} c_{2\downarrow}^+), \quad (3.21)$$

and

$$H_0|\phi_i\rangle = E_0|\phi_i\rangle = 0 \quad (i = 1, 2, 3, 6), \quad H_0|\phi_4\rangle = U|\phi_4\rangle, \quad H_0|\phi_5\rangle = U|\phi_5\rangle, \quad (3.22)$$

$$H_1|\phi_2\rangle = t(|\phi_4\rangle - |\phi_5\rangle). \quad (3.23)$$

From the perturbation theory (time-independent non-degenerate case), we have

$$E_n = E_n^{(0)} + \langle \psi_n^{(0)} | H_1 | \psi_n^{(0)} \rangle + \langle \psi_n^{(0)} | H_1 (E_n^{(0)} - H_0)^{-1} P H_1 | \psi_n^{(0)} \rangle, \quad (3.24)$$

where P is the complementary projection operator. Here we calculate the second process.

$$H_1(E_0 - H_0)^{-1} P H_1 |\phi_2\rangle \text{ for } |\psi_n^{(0)}\rangle = |\phi_2\rangle. \quad (3.25)$$

Note that $P|\phi_i\rangle = |\phi_i\rangle$ ($i = 1, 2, 3, 6$), $\hat{P}|\phi_4\rangle = |\phi_4\rangle$, $P|\phi_5\rangle = |\phi_5\rangle$, $H_1|\phi_2\rangle = t(|\phi_4\rangle + |\phi_5\rangle)$, and

$H_0|\phi_4\rangle = t(|\phi_4\rangle + |\phi_5\rangle)$. Then we have

$$H_{eff}|\phi_2\rangle = H_1(E_0 - H_0)^{-1} P H_1 |\phi_2\rangle$$

$$= t H_1(E_0 - H_0)^{-1} (|\phi_4\rangle + |\phi_5\rangle) = t H_1(-H_0)^{-1} (|\phi_4\rangle + |\phi_5\rangle) \quad (3.26)$$

or

$$H_{ef}|\phi_2\rangle = -\frac{t}{U} \hat{H}_1 (|\phi_4\rangle + |\phi_5\rangle) = -\frac{2t^2}{U} (|\phi_2\rangle - |\phi_3\rangle). \quad (3.27)$$

Here we use the Dirac notation for the spin exchange operator¹¹

$$\hat{P}_{12} = \frac{1}{2}(1 + \hat{\mathbf{S}}_1 \cdot \hat{\mathbf{S}}_2) = \frac{1}{2}(1 + 4\hat{\mathbf{S}}_1 \cdot \hat{\mathbf{S}}_2), \quad (3.28)$$

where S_1 and S_2 are the spin operators of the 1 and 2 sites. Here we note that

$$\begin{aligned} \frac{2t^2}{U} \left(2\hat{S}_1 \cdot \hat{S}_2 - \frac{1}{2} \right) |\phi_2\rangle &= \frac{2t^2}{U} (\hat{P}_{12} - 1) |1\uparrow, 2\downarrow\rangle \\ &= -\frac{2t^2}{U} (|1\uparrow, 2\downarrow\rangle - |1\downarrow, 2\uparrow\rangle) = \hat{H}_{eff} |\phi_2\rangle \end{aligned} \quad (3.29)$$

or

$$H_{eff} = \frac{4t^2}{U} (\hat{S}_1 \cdot \hat{S}_2 - \frac{1}{4}) = 2J (\hat{S}_1 \cdot \hat{S}_2 - \frac{1}{4}), \quad (3.30)$$

with $J = \frac{2t^2}{U}$.

Thus the effective spin Hamiltonian for 2^N states is given by

$$H_{eff} = 2J \sum_{(i,j)} \hat{S}_i \cdot \hat{S}_j, \quad (3.31)$$

where $J = 2t^2/U > 0$. This Hamiltonian is called an antiferromagnetic Heisenberg Hamiltonian. The summation is taken over the nearest neighbor pairs of spins.

In summary, the resultant spin Hamiltonian is a sum of antiferromagnetic and ferromagnetic interactions,

$$\hat{H}_{total} = 2 \left(\frac{2t^2}{U} - J_{direct} \right) (\hat{S}_1 \cdot \hat{S}_2 + \frac{1}{4}). \quad (3.32)$$

Where J_{direct} is the ferromagnetic interaction (direct exchange interaction).

3.5. Mathematica program: eigenvalue problem for the Hubbard model

Simple case of the Hubbard model, eigenvalue problem

A1={ {0,0,0,0,0,0}, {0,0,0,-t,-t,0}, {0,0,0,-t,-t,0}, {0,-t,-t,U,0,0}, {0,-t,-t,0,U,0}, {0,0,0,0,0,0} }; A1//MatrixForm

$$\begin{pmatrix} 0 & 0 & 0 & 0 & 0 & 0 \\ 0 & 0 & 0 & -t & -t & 0 \\ 0 & 0 & 0 & -t & -t & 0 \\ 0 & -t & -t & U & 0 & 0 \\ 0 & -t & -t & 0 & U & 0 \\ 0 & 0 & 0 & 0 & 0 & 0 \end{pmatrix}$$

eq1=Eigensystem[A1]//Simplify

$$\begin{aligned} &\left\{ \left\{ 0, 0, 0, U, \frac{1}{2} \left(U - \sqrt{16t^2 + U^2} \right), \frac{1}{2} \left(U + \sqrt{16t^2 + U^2} \right) \right\}, \right. \\ &\left\{ \{0, 0, 0, 0, 0, 1\}, \{0, -1, 1, 0, 0, 0\}, \{1, 0, 0, 0, 0, 0\}, \right. \\ &\left\{ 0, 0, 0, -1, 1, 0 \right\}, \left\{ 0, \frac{4t}{-U + \sqrt{16t^2 + U^2}}, \frac{4t}{-U + \sqrt{16t^2 + U^2}}, 1, 1, 0 \right\}, \\ &\left. \left\{ 0, -\frac{4t}{U + \sqrt{16t^2 + U^2}}, -\frac{4t}{U + \sqrt{16t^2 + U^2}}, 1, 1, 0 \right\} \right\} \end{aligned}$$

Eg=eq1[[1,5]]

$$\frac{1}{2} \left(U - \sqrt{16t^2 + U^2} \right)$$

The ground state energy of the system Eg

We use $x = t/U$ and $U = ty$ depending on the magnitudes of U and t .

Eg11=Eg/.{t→ U x} //Simplify[#,U>0] &

```

1
2
2 (U - U sqrt(1 + 16 x^2))
Eg12=Series[Eg11,{x,0,3}]/Normal
-4 U x^2
Eg21=Eg/.{U->t y} //Simplify[#,t>0]&
General ::spell1 : Possible spelling error : new
symbol name "Eg21" is similar to existing symbol "Eg12". More..
1
2
2 t (y - sqrt(16 + y^2))
Eg22=Series[Eg21,{y,0,3}]/Normal
-2 t + t y / 2 - t y^2 / 16

```

Eigenkets

ϕ_1 (E = 0), ϕ_2 (E = 0), ϕ_3 (E = 0), ϕ_4 (E = U),

ϕ_5 (E=E5)

ϕ_6 (E=E6)

$$\phi_1 = \frac{\text{eq1}[[2, 1]]}{\sqrt{\text{eq1}[[2, 1]] \cdot \text{eq1}[[2, 1]]}}$$

$$\{0, 0, 0, 0, 0, 1\}$$

$$\phi_2 = \frac{\text{eq1}[[2, 2]]}{\sqrt{\text{eq1}[[2, 2]] \cdot \text{eq1}[[2, 2]]}}$$

$$\{0, -\frac{1}{\sqrt{2}}, \frac{1}{\sqrt{2}}, 0, 0, 0\}$$

$$\phi_3 = \frac{\text{eq1}[[2, 3]]}{\sqrt{\text{eq1}[[2, 3]] \cdot \text{eq1}[[2, 3]]}}$$

$$\{1, 0, 0, 0, 0, 0\}$$

$$\phi_4 = \frac{\text{eq1}[[2, 4]]}{\sqrt{\text{eq1}[[2, 4]] \cdot \text{eq1}[[2, 4]]}}$$

$$\{0, 0, 0, -\frac{1}{\sqrt{2}}, \frac{1}{\sqrt{2}}, 0\}$$

ϕ_5 and ϕ_6 are not normalized.

We consider the special case for ϕ_5 and ϕ_6 in the limit of $U \gg t$ and $U \ll t$.

```

phi51=eq1[[2,5]]
{0, 4 t / (-U + sqrt(16 t^2 + U^2)), 4 t / (-U + sqrt(16 t^2 + U^2)), 1, 1, 0}
phi52=phi51/.{t->U
x} //Simplify[#,U>0]& //Series[#, {x,0,3}]& //Normal
{0, 1/(2 x) + 2 x - 8 x^3, 1/(2 x) + 2 x - 8 x^3, 1, 1, 0}
phi53=phi51/.{U->t
y} //Simplify[#,t>0]& //Series[#, {y,0,3}]& //Normal
{0, 1 + Y/4 + Y^2/32, 1 + Y/4 + Y^2/32, 1, 1, 0}
phi61=eq1[[2,6]]
{0, -4 t / (U + sqrt(16 t^2 + U^2)), -4 t / (U + sqrt(16 t^2 + U^2)), 1, 1, 0}
phi62=phi61/.{t->U
x} //Simplify[#,U>0]& //Series[#, {x,0,3}]& //Normal
{0, -2 x + 8 x^3, -2 x + 8 x^3, 1, 1, 0}
phi63=phi61/.{U->t
y} //Simplify[#,t>0]& //Series[#, {y,0,3}]& //Normal

```

$$\left\{0, -1 + \frac{Y}{4} - \frac{Y^2}{32}, -1 + \frac{Y}{4} - \frac{Y^2}{32}, 1, 1, 0\right\}$$

Plot of energy levels

```
Energy =  $\frac{1}{U}$  eq1[[1]] /. {t -> Ux} // Simplify[#, U > 0] &
{0, 0, 0, 1,  $\frac{1}{2} \left(1 - \sqrt{1 + 16x^2}\right), \frac{1}{2} \left(1 + \sqrt{1 + 16x^2}\right)}$ 
Plot[Evaluate[Energy], {x, 0, 1}, PlotStyle -> Table[Hue[0.2
i], {i, 0, 5}], Prolog -> AbsoluteThickness[3],
AxesLabel -> {"t/U", "E/U"}, Background -> GrayLevel[0.7]]
```

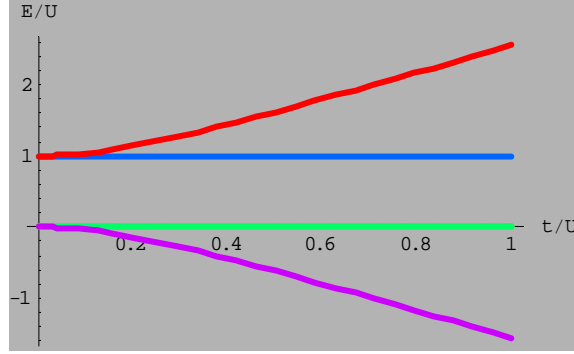


Fig.7 The normalized energy levels E/U as a function of t/U . $|\psi_1\rangle, |\psi_2\rangle, |\psi_3\rangle$ (green), $|\psi_4\rangle$ (blue), $|\psi_5\rangle$ (purple), and $|\psi_6\rangle$ (red).

4. Superexchange interaction (first approach by Anderson,⁵ 1950)

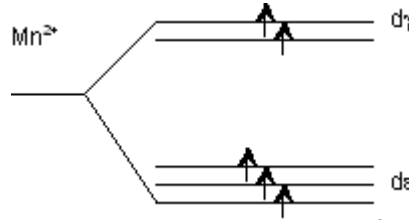


Fig.8 Electron configuration of Mn^{2+} with $(3d)^5$.

The idea can be illustrated by two Mn^{2+} ions and one intervening O^{2-} (White¹⁷) The $\text{Mn}^{2+}(\text{A}) - \text{O}^{2-} - \text{Mn}^{2+}(\text{B})$ are arranged along the one axis, forming a 180° position. There are two spins in the O^{2-} site (the up-spin state $|+\rangle$ and down-spin state $|-\rangle$). Because of the overlap of wave functions, one of p electrons (with down-spin state $|-\rangle$) from the O^{2-} hops over to one of Mn^{2+} ions (A). (in Figs.8, 9, and 10) we assume that a part of one electron hops). Note that only the down-state electron of p -electrons can move to the Mn^{2+} site (A). The remaining unpaired p electron on the O^{2-} site then enters into a direct exchange with the other Mn^{2+} ion (B) with an exchange interaction J . The resultant interaction between the Mn^{2+} ions coupled through O^- ions is antiferromagnetic.

Here we evaluate the magnitude of effective interaction between $\text{Mn}^{2+}(\text{A})$ and $\text{Mn}^{2+}(\text{B})$. We introduce two parameters; (i) the energy matrix element t for shifting p -electron to A and (ii) the increase of energy ($= \xi$) for the shift of p -electron to $\text{Mn}^{2+}(\text{A})$. Then

probability of the above process is evaluated as $(t/\xi)^2$, where $\xi = E_d - E_p$. The resultant exchange energy arising from a mixture between ground state and excited state, is $J(t/\xi)^2$. The same thing happens for the case when one of p electrons (with down-spin state $|-\rangle$) from the O^{2-} hops over to one of Mn^{2+} ions (B). So the resultant exchange energy is given by $2Jt^2/(\xi)^2$. When S_1 and S_2 are spins of Mn^{2+} ions (A and B), the superexchange is described by

$$E_{ex} = -2J'S_1 \cdot S_2, \quad (4.1)$$

where $J' = Jt^2/(\xi^2 S^2)$. When $J' < 0$, S_1 and S_2 are antiparallel, favoring the antiferromagnetic spin arrangement.

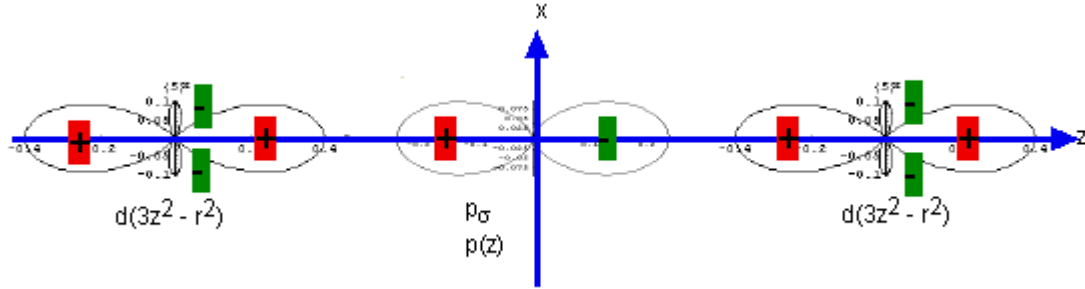


Fig.9 180° configuration

or

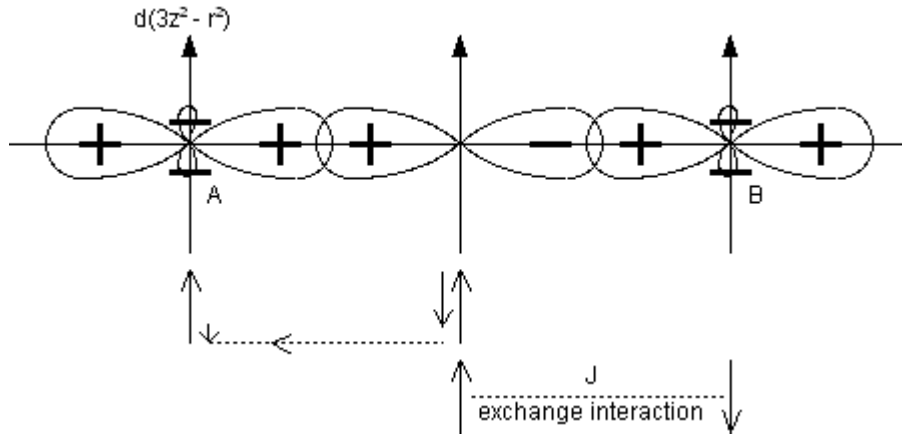


Fig.10 Schematic diagram of the 180° configuration.

5. Superexchange interaction: revised approach

5.1 Molecular orbital due to d - p mixing (P.W. Anderson,⁶ 1959)

It was realized that the original theory (above mentioned) became involved in increasing uncertainties and complexities. The exchange effect appears in a third order of the perturbation theory. One encountered some difficulty. This perturbation theory is poorly convergent. The early terms which do not lead to magnetic effects are rather large.

The basic idea of Anderson⁶ (1959) is simple. We use the following model of the molecular orbital to explain this idea. We consider a $Ni^{2+} (F^-)_6$ octahedron, and consider

the z -axis to lie along one Ni^{2+} - F- bond. The p_σ orbital, of the z symmetry, and the p_π , x and y . It is clear that a covalent bond between the p_σ ($p(z)$) and $d(3z^2 - r^2)$ along the z axis could be formed. The appropriate matrix element to cause this bond does not exist, but, of course, that the d function is considerably higher than the p_σ function in energy and that therefore the best bonding function contains only a relatively small admixture γ of $d(3z^2 - r^2)$.

$$\psi_{\text{bonding}} \approx \psi_{p_\sigma} + \gamma_\sigma \psi_{d(3z^2 - r^2)} \quad (5.1)$$

This bonding function is expected to contain two electrons, the two which originally occupied p_σ ($p(z)$) on the F ion. Now the only wavefunction which is left for the magnetic electrons to occupy is the corresponding antibonding function

$$\psi_{\text{antibonding}} \approx \psi_{d(3z^2 - r^2)} - (\gamma_\sigma + S_\sigma) \psi_{p_\sigma} \quad (5.2)$$

which is orthogonal to ψ_{bonding} : $\langle \psi_{\text{bonding}} | \psi_{\text{antibonding}} \rangle = 0$. Here S_σ is the overlap integral

$$S_\sigma = \int \psi_{d(3z^2 - r^2)}^* \psi_{p_\sigma} d\mathbf{r}. \quad (5.3)$$

The energy of ψ_{bonding} is lower than that of $\psi_{\text{antibonding}}$. There will be a corresponding energy shift in this orbital relative to $d(3z^2 - r^2)$,

$$\Delta E_\sigma = E_{AB} - E_d = \gamma_\sigma^2 (E_d - E_p) = \gamma_\sigma^2 \xi. \quad (5.4)$$

(see 5.4 for the derivation).

5.2 Slater wavefunctions due to the d - p orbital mixing.

We now consider the d - p mixing for the wavefunctions in the system of three-electrons. When the Hamiltonian depends on the spin operators, the wavefunction of the three electrons cannot be described by a product of spatial and spin parts of wavefunctions. Suppose that there are three states; $|d_\uparrow\rangle$, $|p_\uparrow\rangle$ and $|p_\downarrow\rangle$, where p is one of p_x , p_y , p_z orbitals, and d is one of d_γ (ϵ_g) and d_ϵ (t_{2g}) orbitals, and the arrows denote the spin-up and down-states. It is well described by the Slater determinant (Kanamori¹⁸)

$$\psi(1,2,3) = \frac{1}{\sqrt{N}} \left(\begin{vmatrix} d_\uparrow(1) & d_\uparrow(2) & d_\uparrow(3) \\ p_\uparrow(1) & p_\uparrow(2) & p_\uparrow(3) \\ p_\downarrow(1) & p_\downarrow(2) & p_\downarrow(3) \end{vmatrix} + \lambda' \begin{vmatrix} d_\uparrow(1) & d_\uparrow(2) & d_\uparrow(3) \\ p_\uparrow(1) & p_\uparrow(2) & p_\uparrow(3) \\ d_\downarrow(1) & d_\downarrow(2) & d_\downarrow(3) \end{vmatrix} \right), \quad (5.5)$$

where 1, 2, and 3 are position of each electron and spin-coordinates. The second determinant represents the electron configuration after the charge transfer $|p_\downarrow\rangle \rightarrow |d_\downarrow\rangle$.

Using the general property of the determinant (purely mathematics), the above equation can be rewritten as

$$\psi(1,2,3) = \frac{1}{\sqrt{N}} \begin{vmatrix} d_\uparrow(1) & d_\uparrow(2) & d_\uparrow(3) \\ p_\uparrow(1) & p_\uparrow(2) & p_\uparrow(3) \\ p_\downarrow(1) + \lambda' d_\downarrow(1) & p_\downarrow(2) + \lambda' d_\downarrow(2) & p_\downarrow(3) + \lambda' d_\downarrow(3) \end{vmatrix} \quad (5.6)$$

This is also rewritten as

$$\psi(1,2,3) = \frac{1}{\sqrt{N}} \begin{pmatrix} d_{\uparrow}(1) - \lambda p_{\uparrow}(1) & d_{\uparrow}(2) - \lambda p_{\uparrow}(2) & d_{\uparrow}(3) - \lambda p_{\uparrow}(3) \\ p_{\uparrow}(1) + \lambda' d_{\uparrow}(1) & p_{\uparrow}(2) + \lambda' d_{\uparrow}(2) & p_{\uparrow}(3) + \lambda' d_{\uparrow}(3) \\ p_{\downarrow}(1) + \lambda' d_{\downarrow}(1) & p_{\downarrow}(2) + \lambda' d_{\downarrow}(2) & p_{\downarrow}(3) + \lambda' d_{\downarrow}(3) \end{pmatrix}, \quad (5.7)$$

where N is the normalization factor and λ is an arbitrary constant. We choose λ such that $|d\rangle - \lambda|p\rangle$ and $|p\rangle + \lambda'|d\rangle$ are orthogonal.

$$(\langle p| + \lambda'\langle d|)(|d\rangle - \lambda|p\rangle) = 0, \quad (5.8)$$

or

$$\langle p|d\rangle - \lambda + \lambda' - \lambda\lambda'\langle p|d\rangle^* = 0. \quad (5.9)$$

If λ , λ' , and $\langle p|d\rangle$ are real, we have

$$\lambda' = \frac{-S + \lambda}{1 - \lambda S} \approx -S + \lambda, \quad (5.10)$$

where $S = \langle p|d\rangle$ is the overlap integral. We consider two states; $|d\rangle - \lambda|p\rangle$, $|p\rangle + \lambda'|d\rangle$. The state $|d\rangle - \lambda|p\rangle$ is an antibonding orbital (higher energy) and $|p\rangle + \lambda'|d\rangle$ is a bonding orbital (lower energy). In the three-electrons configuration, one electron is in the state $|d\rangle - \lambda|p\rangle$, and two electrons are in the state $|p\rangle + \lambda'|d\rangle$. In the bonding orbital, the resultant spin is equal to zero since two spins (up and down state) would cancel out each other. The spin in the antibonding orbital $|d\rangle - \lambda|p\rangle$ is responsible for the spin distribution of the system.

5.3 Evaluation of superexchange interaction

In the above picture of the molecular orbital, the spin of magnetic ion is located on the orbit given by $\psi_{antibonding}$ which extends over the negative ion. This magnetic ion interacts with the magnetic ion on the other side through a direct exchange interaction. The exchange interaction between the magnetic d -electrons is expressed by

$$-2J_{eff}\hat{\mathbf{S}}_i \cdot \hat{\mathbf{S}}_j, \quad (5.11)$$

where the effective interaction is given by

$$J_{eff} = 2\lambda^2(J_{pd} + W_{pd}), \quad (5.12)$$

where J_{pd} is the direct exchange interaction and $W_{pd} (= -t^2/U)$ is the exchange interaction due to the charge transfer. Here we use the factor of 2 since two magnetic ions are equivalent and no change occurs in the magnetic property, even if the role of one magnetic ion can be replaced by that of the other magnetic ion.

5.4 Simple model of p - d mixing

A. Eigenvalue problem

We now consider a simple eigenvalue problem for the non-degenerate case. \hat{H} is the Hamiltonian leading to the p - d mixing.

$$\begin{aligned} \hat{H}|d\rangle &= E_d|d\rangle + t|p\rangle \\ \hat{H}|p\rangle &= t|d\rangle + E_p|p\rangle \end{aligned} \quad (5.13)$$

The eigenvalue problem is given by

$$\hat{H}|\psi\rangle = E|\psi\rangle, \quad (5.14)$$

$$|\psi\rangle = C_d|d\rangle + C_p|p\rangle. \quad (5.15)$$

The matrix of \hat{H} is given by

$$\hat{H} = \begin{pmatrix} E_d & t \\ t & E_p \end{pmatrix}. \quad (5.16)$$

The energy eigenvalues are determined from the following quadratic equation

$$(E_d - E)(E_p - E) - t^2 = 0. \quad (5.17)$$

The bonding state is given by

$$|\psi_B\rangle = -\frac{2t}{\xi + \sqrt{4t^2 + \xi^2}}|d\rangle + |p\rangle \approx |p\rangle - \frac{t}{\xi}|d\rangle, \quad (5.18)$$

with the energy eigenvalue,

$$E_B = \frac{E_d + E_p - \sqrt{(E_d - E_p)^2 + 4t^2}}{2} = \frac{E_d + E_p}{2} - \frac{1}{2}\sqrt{\xi^2 + 4t^2}, \quad (5.19)$$

or

$$E_B = E_p + \frac{\xi}{2} - \frac{1}{2}\sqrt{\xi^2 + 4t^2} = E_p - \frac{t^2}{\xi} + \frac{t^4}{\xi^3} + \dots, \quad (5.20)$$

where $\xi = E_d - E_p$. The antibonding state is given by

$$|\psi_{AB}\rangle = |d\rangle + \frac{2t}{\xi + \sqrt{4t^2 + \xi^2}}|p\rangle \approx |d\rangle + \frac{t}{\xi}|p\rangle, \quad (5.21)$$

with the energy eigenvalue

$$E_{AB} = \frac{E_d + E_p + \sqrt{(E_d - E_p)^2 + 4t^2}}{2} = \frac{E_d + E_p}{2} + \frac{1}{2}\sqrt{\xi^2 + 4t^2}, \quad (5.22)$$

or

$$E_{AB} = E_d - \frac{\xi}{2} + \frac{1}{2}\sqrt{\xi^2 + 4t^2} = E_d + \frac{t^2}{\xi} - \frac{t^4}{\xi^3} + \dots \quad (5.23)$$

We define the energy difference ΔE given by

$$\Delta E = E_{AB} - E_d = E_p - E_B = -\frac{\xi}{2} + \frac{1}{2}\sqrt{\xi^2 + 4t^2} = \frac{t^2}{\xi} - \frac{t^4}{\xi^3} + \dots \quad (5.24)$$

or

$$\Delta E \approx \frac{t^2}{\xi} = \xi \frac{t^2}{\xi^2} = \xi \gamma^2, \quad (5.25)$$

where $\gamma = t/\xi$ and $\xi = E_d - E_p$.

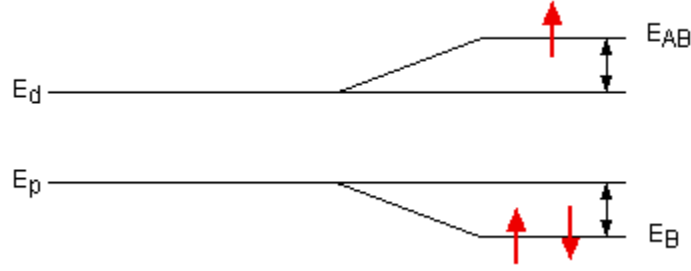


Fig.11 Energy levels E_d and E_p for the d and p orbitals, E_{AB} and E_B for the antibonding and bonding molecular orbitals.

B. Perturbation approach

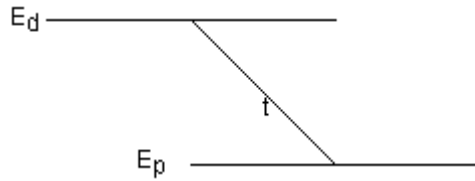


Fig.12 Energy levels E_d and E_p for the d and p orbitals before perturbation.

We apply the perturbation theory to this problem (p - d mixing), where $\xi = E_d - E_p \gg t$.

$$\hat{H}_0|d\rangle = E_d|d\rangle, \quad \hat{H}_0|p\rangle = E_p|p\rangle, \quad (5.26)$$

$$\hat{H}_1|d\rangle = t|p\rangle, \quad \hat{H}_1|p\rangle = t|d\rangle. \quad (5.27)$$

The energy of the anti-bonding and bonding states is described by

$$E_{AB} = E_d + \frac{\langle d|\hat{H}_1|p\rangle\langle p|\hat{H}_1|d\rangle}{(E_d - E_p)} = E_d + \frac{t^2}{E_d - E_p} = E_d + \frac{t^2}{\xi}, \quad (5.28)$$

$$E_B = E_p + \frac{\langle p|\hat{H}_1|d\rangle\langle d|\hat{H}_1|p\rangle}{(E_p - E_d)} = E_p - \frac{t^2}{E_d - E_p} = E_p - \frac{t^2}{\xi}. \quad (5.29)$$

The energy difference ΔE is given by

$$\Delta E = E_{AB} - E_d = E_B - E_d = \frac{t^2}{E_d - E_p} = \frac{t^2}{\xi}, \quad (5.30)$$

$$|\psi_{AB}\rangle = |d\rangle + |p\rangle \frac{\langle p|\hat{H}_1|d\rangle}{(E_d - E_p)} = |d\rangle + \frac{t}{E_d - E_p}|p\rangle = |d\rangle + \frac{t}{\xi}|p\rangle, \quad (5.31)$$

$$|\psi_B\rangle = |p\rangle + |d\rangle \frac{\langle d|\hat{H}_1|p\rangle}{(E_p - E_d)} = |p\rangle - \frac{t}{E_d - E_p}|d\rangle = |p\rangle - \frac{t}{\xi}|d\rangle, \quad (5.32)$$

Then the bonding state is described by $|\psi_B\rangle = |p\rangle - \gamma|d\rangle$. Then the energy difference is

rewritten as $\Delta E = \frac{t^2}{\xi} = \frac{t^2}{\xi^2} \xi = \gamma^2 \xi$, where $\gamma = t/\xi$ and $\xi = E_d - E_p$.

C. Mathematica program for the case A

Exact solution of the eigenvalue problem

$$\psi = c_1 \psi_d + c_2 \psi_p$$

```
H1={{Ed,t},{t,Ep}}
{{Ed,t},{t,Ep}}
eq1=Eigensystem[H1]
{{1/2 (Ed+Ep - Sqrt[Ed^2-2EdEp+Ep^2+4t^2]),
 1/2 (Ed+Ep + Sqrt[Ed^2-2EdEp+Ep^2+4t^2])},
{{- (Ed+Ep + Sqrt[Ed^2-2EdEp+Ep^2+4t^2])/(2t), 1},
{- (Ed+Ep - Sqrt[Ed^2-2EdEp+Ep^2+4t^2])/(2t), 1}}}]
rule1={Ed->Ep+xi}
{Ed->Ep+xi}
```

Antibonding state

$$\xi = E_d - E_p$$

```
phi1={1, 1/(- (Ed+Ep - Sqrt[Ed^2-2EdEp+Ep^2+4t^2])/(2t))} // Simplify
{1, 1/(Ed - Ep + Sqrt[Ed^2-2EdEp+Ep^2+4t^2])}
psiAB=phi1/.rule1//FullSimplify
{1, 1/(xi + Sqrt[4t^2+xi^2])}
```

Bonding state

```
phi2={- (Ed+Ep + Sqrt[Ed^2-2EdEp+Ep^2+4t^2])/(2t), 1}
{- (Ed+Ep + Sqrt[Ed^2-2EdEp+Ep^2+4t^2])/(2t), 1}
psiB=phi2/.rule1//FullSimplify
{xi - Sqrt[4t^2+xi^2]/(2t), 1}
psiB1={-2t/(xi + Sqrt[4t^2+xi^2]), 1}
{-2t/(xi + Sqrt[4t^2+xi^2]), 1}
psiAB.psiB//Simplify
0
```

The energy of antibonding state

```
EAB=eq1[[1,2]]/.rule1//Simplify
1/2 (2Ep+xi + Sqrt[4t^2+xi^2])
Series[EAB,{t,0,4]}//Simplify[#,xi>0]& //Normal
Ep - t^4/xi^3 + t^2/xi + xi
```

The energy of bonding state

```
EB=eq1[[1,1]]/.rule1//Simplify
```

$$\frac{1}{2} \left(2 E_P + \xi - \sqrt{4 t^2 + \xi^2} \right)$$

```
Series[EB, {t, 0, 4}] // Simplify[#, ξ > 0] & // Normal
```

$$E_P + \frac{t^4}{\xi^3} - \frac{t^2}{\xi}$$

The energy difference between the antibonding and bonding states

```
DEN=EAB-EB/.rule1//Simplify
```

$$\sqrt{4 t^2 + \xi^2}$$

6 Molecular orbitals

6.1. hybridization of $2s$ and $2p(z)$ orbitals

Before discussing the molecular orbitals of $2p$ and $3d$ electrons, first we consider the simple case, the hybridization of $2s$ orbital and $2p(z)$ orbital. The $2s$ orbital is spherically symmetric about the origin, while the $2p(z)$ orbital has a dumbbell-shape whose rotation axis is the z axis. We consider the wavefunction given by $|\psi\rangle = |2p(z)\rangle + \lambda|2s\rangle$, where λ is chosen as a parameter. The electronic density of the state $|2s\rangle$ is positive in both the $+z$ and $-z$ directions, while the electronic density of the state $|2p(z)\rangle$ is positive in the $+z$ direction and negative in the $-z$ direction. For $\lambda > 0$, the electronic density of $|\psi\rangle$ has a lopsided orbital. The amplitude in the $+z$ axis side is larger than that in the $-z$ direction. For $\lambda < 0$, on the other side, the amplitude in the $-z$ axis side is larger than in the $+z$ axis side. The shape depends on the sign of λ . Figure 13 shows the result of the calculation for the angular distribution of $|\psi\rangle$ using Mathematica (SphericalPlot3D), where $\lambda = -0.3, 0$, and 0.3 . Such a phenomenon is called the hybridization. Note that in the Baym's textbook,¹² he used the wavefunction given by $|\psi\rangle = |2s\rangle + \lambda|2p(z)\rangle$ with $\lambda = -0.5 - 0.5$ which is different from our notation. We tried to calculate the electronic density using Mathematica. We could not reproduce the result which he showed in his textbook.

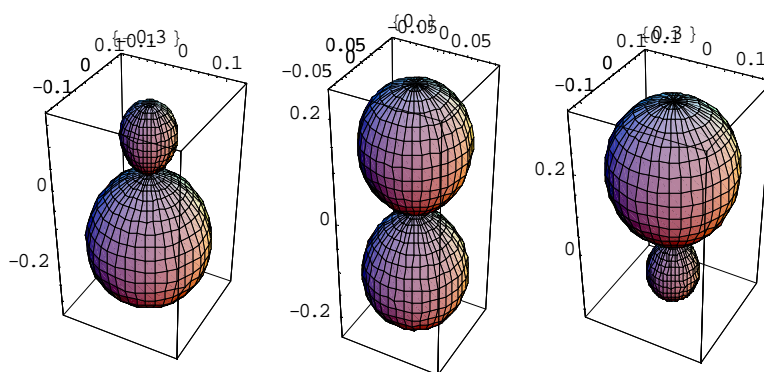


Fig.13 3D polar representation of $|\psi\rangle = |2p(z)\rangle + \lambda|2s\rangle$ with $\lambda = -0.3, 0$, and 0.3

6.2 Mixing of $d\gamma p_\sigma$ orbitals and $d\gamma p_\sigma$

A. Antibonding molecular orbital of $d(3z^2 - r^2)$ and $p(z)$ ($= p_\sigma$)

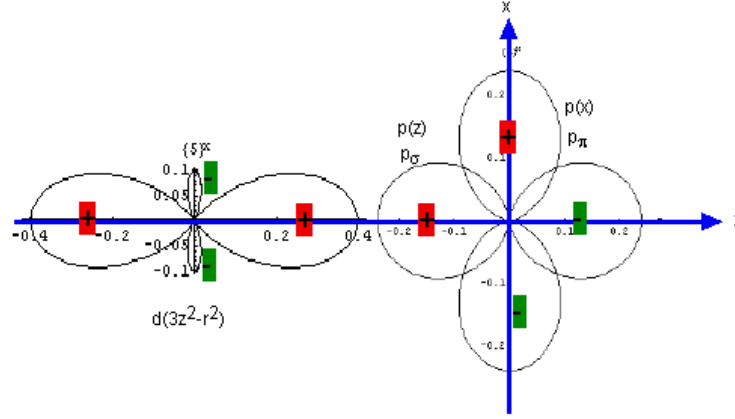


Fig.14 Symmetry relation of $d(3z^2 - r^2)$ ($= d\gamma$ or e_g), $p(z)$ ($= p_\sigma$) and $p(x)$ ($= p_\pi$).

Here we consider the antibonding molecular orbital $|\psi\rangle = |d(3z^2 - r^2)\rangle - \lambda |p(z)\rangle$ which occurs as a result of the p - d mixing. The $d(3z^2 - r^2)$ orbital has a dumbbell shape whose rotation axis is the z axis, and a small circular disk-shape around the origin. The electron density of the dumbbell in the $d(3z^2 - r^2)$ orbital is positive in both the $+z$ and $-z$ directions. The electron density of the circular disk shape in the $d(3z^2 - r^2)$ orbital is negative in both $+x$ and $-x$ directions. The $p(z)$ ($= p_\sigma$) orbital has a dumbbell shape whose rotation axis is the z axis. The electronic density of the state $p(z)$ is negative in the $+z$ -direction and positive in the $-z$ direction. For $\lambda < 0$, the electronic density of $|\psi\rangle$ has a lopsided orbital. The amplitude of the dumbbell in the $+z$ axis side is much larger than that in the $-z$ direction. For $\lambda < 0$, the amplitude of the dumbbell in the $-z$ axis side is much larger than in the $+z$ axis side. The shape of the lopsided orbital depends on the sign of λ . In contrast, the circular disk-shape around the origin is almost independent of λ . Figure 15 shows the results of the calculation for the angular distribution of $|\psi\rangle$ using Mathematica (SphericalPlot3D), where $\lambda = -0.4, 0$, and 0.4 . In conclusion, there is a strong covalency of $d\gamma$ and p_σ orbitals along the direction connecting between d and p electrons (the z axis in the present case). We may say that there is an overlap of wavefunctions between $d\gamma$ and p_σ . The orbits $d\gamma$ and p_σ are not orthogonal, $d\gamma \not\perp p_\sigma$.

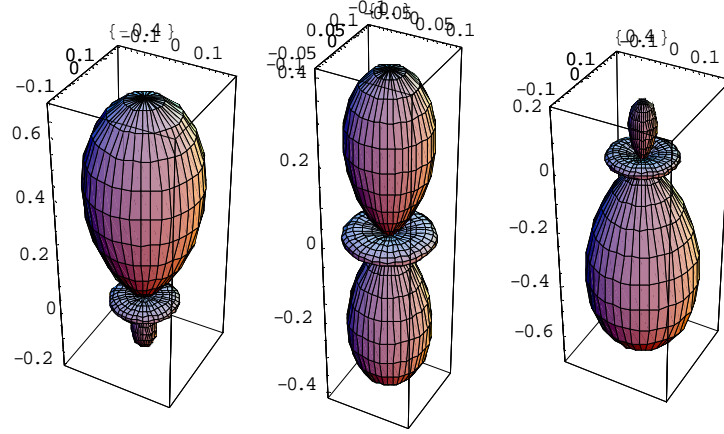


Fig.15 3D polar representation of $|\psi\rangle = |d(3z^2 - r^2)\rangle - \lambda|p(z)\rangle$ with $\lambda = -0.4, 0$, and 0.4 .

B. Antibonding molecular orbitals of $d(3z^2 - r^2)$ and $p(x)$ ($= p_\pi$)

Here we consider the antibonding molecular orbital $|\psi\rangle = |d(3z^2 - r^2)\rangle - \lambda|p(x)\rangle$. The $p(x)$ ($= p_\pi$) orbital has a dumbbell shape whose rotation axis is the x axis. The electronic density of the state $p(x)$ ($= p_\pi$) is positive in the $+x$ direction and negative in the $-x$ direction. The dumbbell shape almost remains unchanged for $\lambda = -0.4, 0$, and 0.4 . In contrast, the circular disk-shape is strongly dependent on the value of λ . The center of the circular disc shifts along the $-x$ direction for $\lambda > 0$ and along the $+x$ direction. Figure 16 shows the electronic density of $|\psi\rangle$ calculated using Mathematica (SphericalPlot3D), where $\lambda = -0.4, 0$, and 0.4 . In conclusion, there is a weak covalency between $d\gamma$ and p_π orbitals along the direction connecting between d and p electrons (the z axis in the present case). We may say that there is no overlap between $d\gamma$ and p_π . $d\gamma \perp p_\pi$.

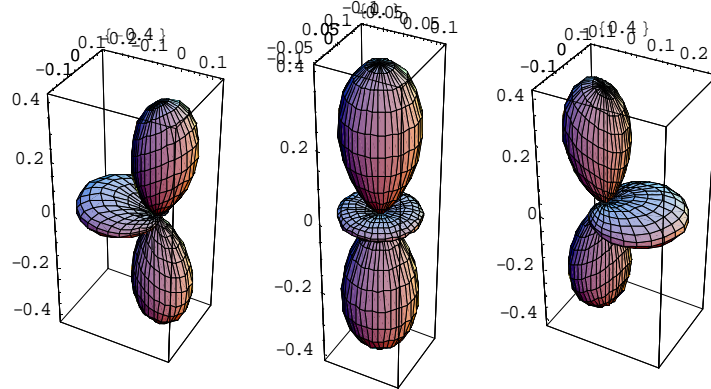


Fig.16 3D polar representation of $|\psi\rangle = |d(3z^2 - r^2)\rangle - \lambda|p(x)\rangle$ with $\lambda = -0.4, 0$, and 0.4 .

6.2 Mixing of $d\varepsilon-p_\sigma$ orbitals and $d\varepsilon-p_\pi$

A. Antibonding molecular orbital of $d(zx)$ and $p(z)$ ($= p_\sigma$)

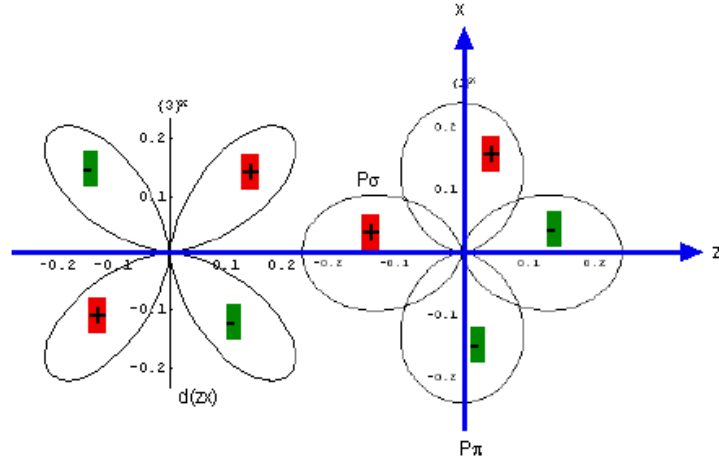


Fig.17 Symmetry relation of $d(zx)$ ($= d\varepsilon$ or t_{2g}), $p(z)$ ($= p_\sigma$) and $p(x)$ ($= p_\pi$).

We consider the antibonding molecular orbital $|\psi\rangle = |d(zx)\rangle - \lambda|p(z)\rangle$. The $d(zx)$ ($= d\varepsilon$) orbital has a clover shape with 4 leaves in the z - x plane. The electronic density of the $d(zx)$ orbital is positive for the leaves in the first and third quadrants and negative in the second and fourth quadrants. The $p(z)$ ($= p_\sigma$) orbital has a dumbbell shape whose rotation axis is the z axis. The electronic density of the state $p(x)$ ($= p_\pi$) is positive in the $+x$ -direction and negative in the $-x$ direction. Figure 18 shows the electronic density of $|\psi\rangle = |d(zx)\rangle - \lambda|p(z)\rangle$ calculated using Mathematica (SphericalPlot3D), where $\lambda = -0.4$, 0 , and 0.4 . For $\lambda > 0$, the region of the leaves of the third and fourth quadrants in the z - x plane becomes large, while the region of the leaves of the first and second quadrants becomes small. For $\lambda < 0$, the region of the leaves of the third and fourth quadrants in the z - x plane becomes small, while the region of the leaves of the first and second quadrants becomes large. Note that for $\lambda = 0$, the electronic density of $|d(zx)\rangle$ is equal to zero on the z axis. In conclusion, there is a weak covalency between $d\varepsilon$ and p_σ orbitals along the x axis, rather than the z axis connecting between d and p electrons. We may say that there is no overlap of wavefunctions between $d\varepsilon$ and p_σ , $d\varepsilon \perp p_\sigma$.

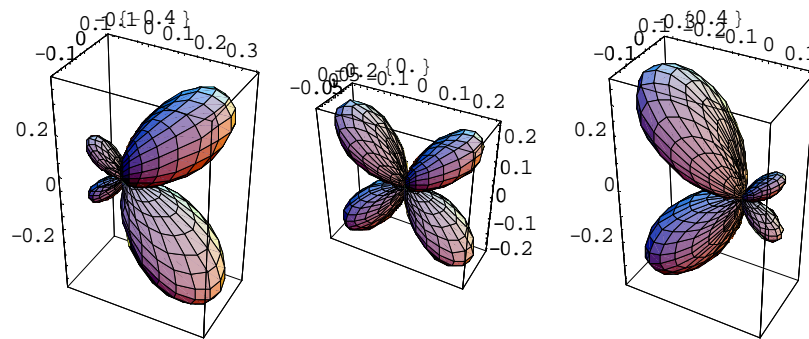


Fig.18 3D polar representation of $|\psi\rangle = |d(zx)\rangle - \lambda|p(z)\rangle$ with $\lambda = -0.4$, 0 , and 0.4 .

B. Antibonding molecular orbital of $d(zx)$ and $p(x)$ ($=p_\pi$)

We consider the antibonding molecular orbital $|\psi\rangle = |d(zx)\rangle - \lambda|p(x)\rangle$. The $p(x)$ ($=p_\pi$) orbital has a dumbbell shape whose rotation axis is the x axis. The electronic density of the state $p(x)$ ($=p_\pi$) is positive in the $+x$ -direction and negative in the $-x$ direction. Figure 19 shows the electronic density of $|\psi\rangle = |d(zx)\rangle - \lambda|p(x)\rangle$ calculated using Mathematica (SphericalPlot3D), where $\lambda = -0.4, 0$, and 0.4 . For $\lambda > 0$, the region of the leaves of the first and fourth quadrants in the z - x plane becomes small, while the region of the leaves of the second and third quadrants becomes large. For $\lambda < 0$, the region of the leaves of the first and fourth quadrants in the z - x plane becomes large, while the region of the leaves of the second and third quadrants becomes small. In conclusion, there is a relatively strong covalency between $d\varepsilon$ and p_π orbitals along the z axis connecting between d and p electrons. We may say that there is overlap of wavefunctions between $d\varepsilon$ and p_π orbitals, $d\varepsilon \nleftrightarrow p_\pi$.

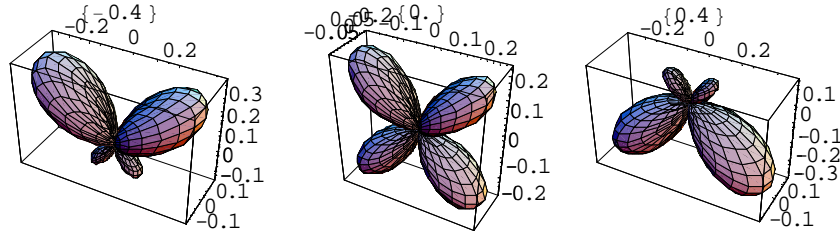


Fig.19 3D polar representation of $|\psi\rangle = |d(zx)\rangle - \lambda|p(x)\rangle$ with $\lambda = -0.4, 0$, and 0.4 .

7. The Goodenough-Kanamori-Anderson rules

7.1 180° and 90° superexchange interactions

A considerably more satisfactory system of semiempirical rules was developed over a period of years by Goodenough⁷ and Kanamori.⁸ The main features of the superexchange interactions are usually explained in terms of the so-called Goodenough-Kanamori-Anderson rules.^{9,10} These rules have the important features of taking into account the occupation of the various d levels as dictated by ligand field theory. According to these rules, a 180° superexchange (the magnetic ion-ligand-magnetic ion angle is 180°) of two magnetic ions with partially filled d shells is strongly antiferromagnetic, whereas a 90° superexchange interaction is ferromagnetic and much weaker. In Appendix, we show the magnetic properties of typical pure spin systems (2D and 3D) which we are interested in.^{19,20}

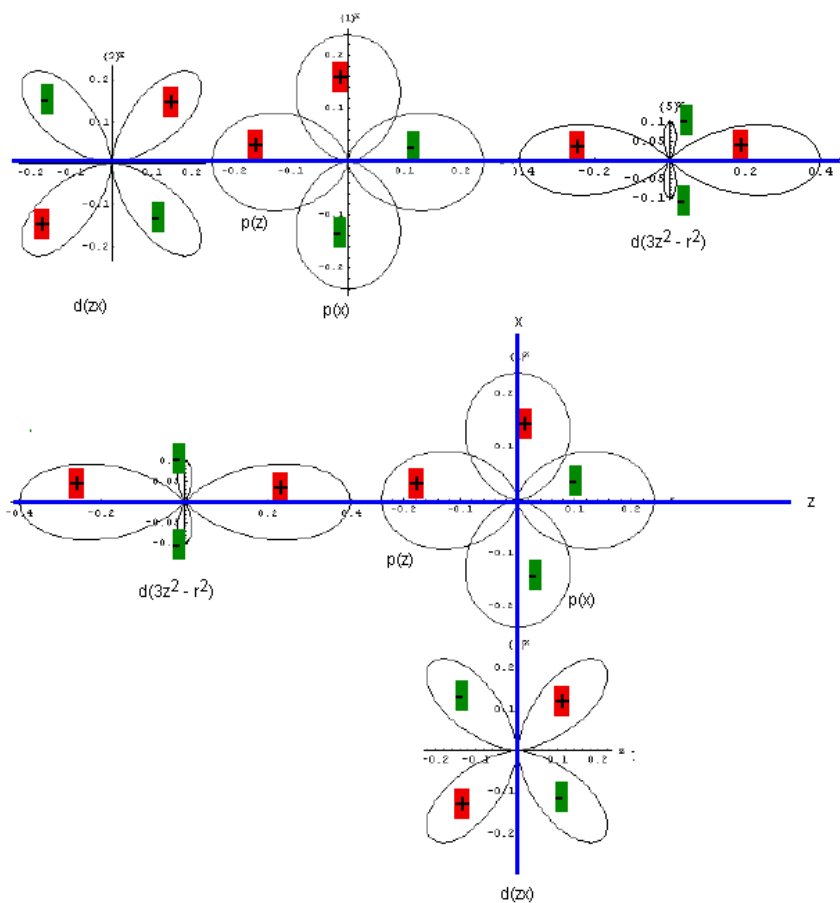


Fig.20 180° and 90° configurations for the 3d orbital-p orbital-3d orbital.

or

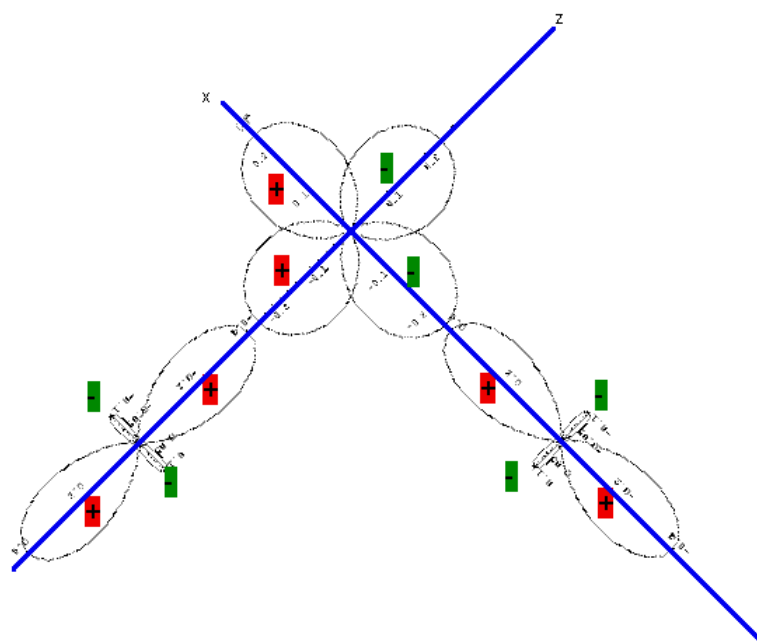


Fig.21 90° configuration for the 3d orbital-p orbital-3d orbital.

7.2 General rules for GKA^{9,10}

These rules seem to explain almost the complete gamut of spin pattern data on a wide variety of substances.⁹

- A. When the two ions have lobes of magnetic orbitals pointing toward each other in such a way that the orbitals would have a reasonably overlap integral, the exchange is antiferromagnetic. There are several subcases.
 - (a) When the lobes are $d(3z^2-r^2)$ type orbitals in the octahedral case, particularly in the 180° position in which these lobes point directly toward a ligand and each other, one obtain particularly large superexchange.
 - (b) When $d(xy)$ orbitals are in the 180° position to each other, so that they can interact via p_π orbitals on the ligand, one again obtain antiferromagnetism.
 - (c) In a 90° ligand situation, when one ion has a $d(3z^2-r^2)$ occupied and the other a $d(xy)$, the p_π for one is the p_σ for the other and one expect strong overlap and thus antiferromagnetic exchange.
- B. When the orbitals are arranged in such a way that they are expected to be in contact but to have no overlap integral- most notably a $d(3z^2-r^2)$ and $d(xy)$ in 180° position, where the overlap is zero by symmetry, the rule gives ferromagnetic interaction (not, however, usually as strong as the antiferromagnetic one).

7.3. Rules of GKA

There are four rules, $d\varepsilon \perp p_\sigma$, $d\gamma \perp p_\pi$, $d\varepsilon \not\perp p_\pi$, $d\gamma \not\perp p_\sigma$, where $d\varepsilon = t_{2g}$ and $d\gamma = e_g$.

A. $d\varepsilon \perp p_\sigma$

The p_σ -orbital does not change its sign when the coordinate axes are rotated around the line connecting these ions. The occupied $d\varepsilon$ -orbitals do change their sign. Therefore the p_σ -orbital is orthogonal to the $d\varepsilon$ -orbital ($d\varepsilon \perp p_\sigma$). This implies that the exchange integral between $d\varepsilon$ and p_σ is positive (ferromagnetic) (see Sec.2.2).

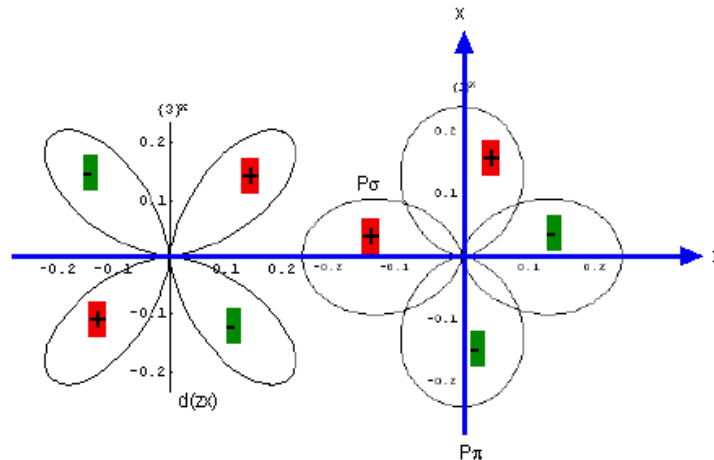


Fig.22 The symmetry relation. $d\varepsilon[d(zx)] \perp p_\sigma[p(z)]$. $d\varepsilon[d(zx)] \not\perp p_\pi[p(x)]$.

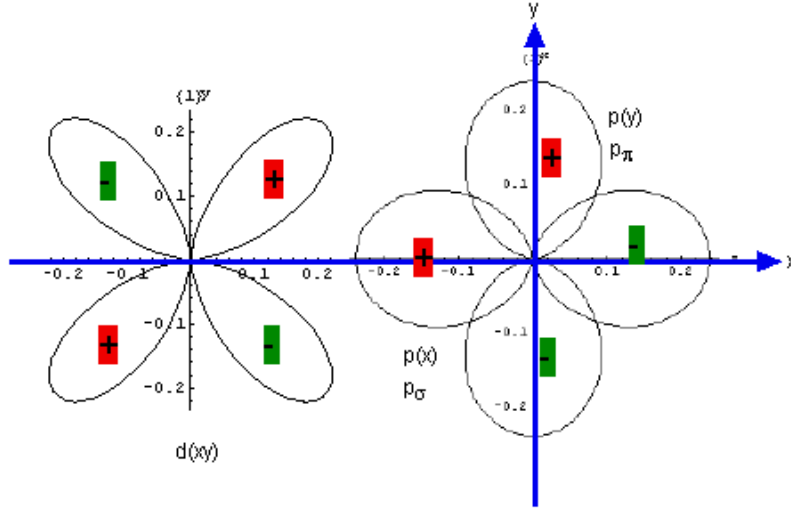


Fig.23 The symmetry relation. $d\varepsilon[d(xy)] \perp p_\sigma[p(x)]$. $d\varepsilon[d(xy)] \not\perp p_\pi[p(y)]$.

B. $d\gamma \not\perp p_\sigma$

The electron transfer, or partial covalence, can only take place between p_σ and $d\gamma$. The orbit $d(3z^2 - r^2)$ does not change sign by rotating the coordinate axes around the x -axis. Therefore a partial covalent bond involving the p_σ -orbital can be formed with the $d\gamma$ orbital; i.e., electron transfer from p_σ can take place to the $d\gamma$ orbital, but not to the $d\varepsilon$ -orbitals. The charge transfer can take place only if the cation and anion orbitals are non-orthogonal. If the cation-anion orbitals are orthogonal, the direct exchange referred to above is positive (ferromagnetic); otherwise it is negative (antiferromagnetic).

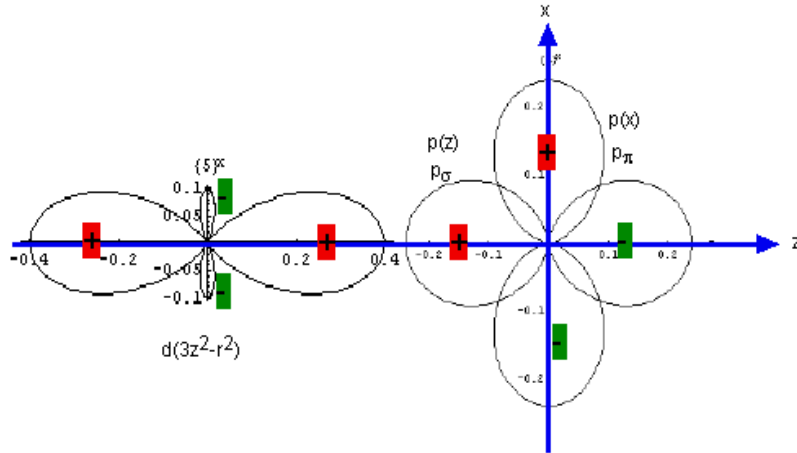


Fig.24 The symmetry relation. $d\gamma[d(3z^2 - r^2)] \not\perp p_\sigma[p(z)]$. $d\gamma[d(3z^2 - r^2)] \perp p_\pi[p(x)]$.

C $d\gamma \perp p_\pi$

Figure 23 shows the symmetry relation between the $d\varepsilon$ -orbital $[d(xy)]$ and the p -orbital $[p(x), p_\sigma$ and $p(y); p_\pi$ orbital]. Figure 25 shows the symmetry relation between the $d\gamma$ -orbital $[d(x^2 - y^2)]$ and the p -orbital $[p(x), p_\sigma$ and $p(y); p_\pi$ orbital]. The p_σ orbital is orthogonal to the $d\varepsilon$ -orbital $[d(xy)]$. But it is not orthogonal to the $d\gamma$ -orbital $[d(x^2 - y^2)]$. There is a principal overlap between these orbitals, leading to the occurrence of the

charge transfer, or partial covalence (so-called σ transfer). On the other hand, the p_π orbital is orthogonal to the $d\gamma$ -orbital [$d(x^2 - y^2)$]. But it is not orthogonal to the $d\varepsilon$ -orbital [$d(xy)$]. There is a principal overlap between these orbitals, leading to the occurrence of the charge transfer (so-called π transfer). Since the orbital overlap involved in the σ transfer is greater than that in the π transfer, processes involving σ transfer are stronger.

In summary we have

$$p_\sigma \perp d\varepsilon(t_{2g}),$$

strong overlap between p_σ and $d\gamma(e_g)$,

$$p_\pi \perp d\gamma(e_g),$$

weak overlap between p_π and $d\varepsilon(t_{2g})$,

The orbit $d\gamma$ [$d(x^2 - y^2)$] is orthogonal to the orbit p_π . So there is no charge transfer between $d\gamma[d(x^2 - y^2)]$ and p_π . The direct exchange is ferromagnetic.

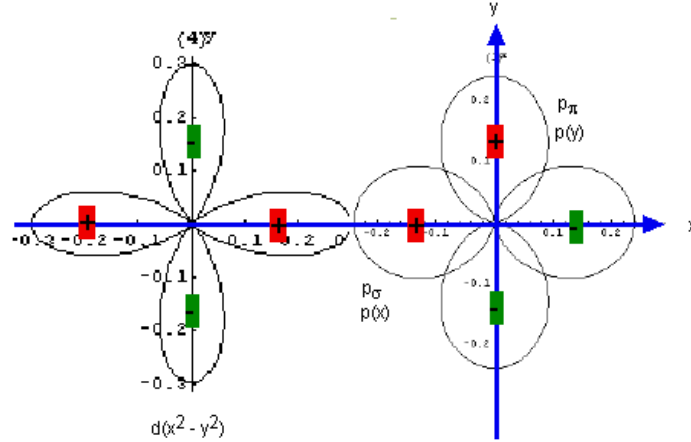


Fig.25 The symmetry relation. $d\gamma[d(x^2-y^2)] \perp p_\pi[p(y)]$. $d\gamma[d(x^2-y^2)] \not\perp p_\sigma[p(x)]$.

D. $d\varepsilon \not\perp p_\pi$

The $d\varepsilon$ - p_π bond should be weaker than the $d\gamma$ - p_σ bond owing to a smaller overlap. The direct exchange interaction is antiferromagnetic.

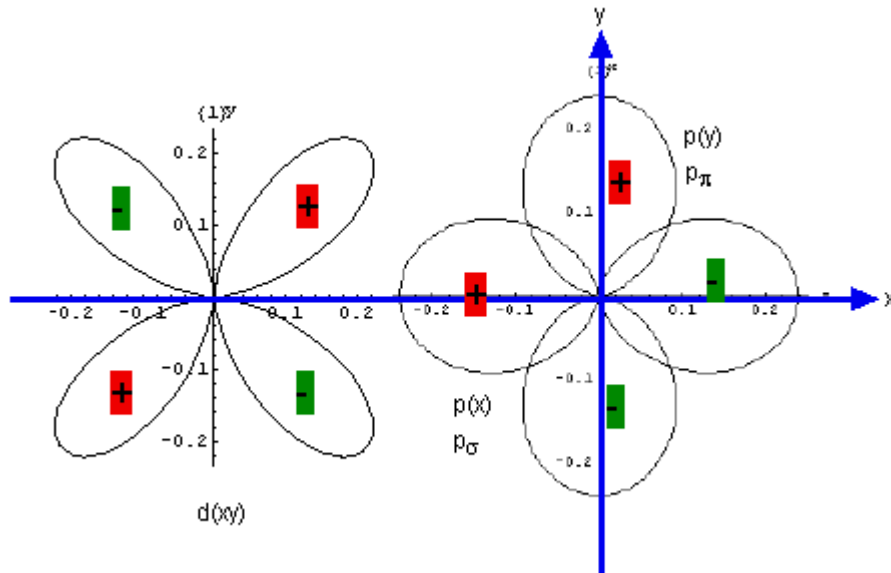


Fig.26 The symmetry relation. $d\varepsilon[d(xy)] \perp p_\sigma[p(x)]$. $d\varepsilon[d(xy)] \not\perp p_\pi[p(y)]$.

Note that σ -transfer is stronger than the π -transfer. the $d\varepsilon$ - p_π bond should be weaker than the $d\gamma$ - p_σ bond owing to a smaller overlap. The $d\gamma$ - s bond has the same property as the $d\gamma$ - p_σ bond, and therefore we shall confine ourselves in the following to the $d\gamma$ - p_σ bond. In fact we have no mean of clearly distinguishing between them, because an electron transfer can generally occur from an s - p hybridized orbital.

The rules obtained are summarized as follows.

- $d\gamma \not\perp p_\sigma \Leftrightarrow$ charge transfer
- $d\gamma \not\perp p_\sigma \Leftrightarrow$ antiferromagnetic (non-orthogonal)
- $d\gamma \perp p_\pi \Leftrightarrow$ no charge transfer
- $d\gamma \perp p_\pi \Leftrightarrow$ ferromagnetic (orthogonal)

- $d\varepsilon \not\perp p_\pi \Leftrightarrow$ charge transfer
- $d\varepsilon \not\perp p_\pi \Leftrightarrow$ antiferromagnetic (non-orthogonal)
- $d\varepsilon \perp p_\sigma \Leftrightarrow$ no charge transfer
- $d\varepsilon \perp p_\sigma \Leftrightarrow$ ferromagnetic (orthogonal)

7.4. GKA rules for the 90° configuration

The rules for the 90° configuration are different from those for the 180° configuration. Here we take an example of the $d\varepsilon$ (cation-1) - p_σ (anion) - $d\varepsilon'$ (cation-2) bond. As is discussed above, the $d\varepsilon$ -orbital of the cation-1 is orthogonal to the p_σ orbital of the anion. The p_σ orbital has a dumbbell shape whose rotation axis is parallel to the direction of the bond between the cation-1 and the anion. For 180° configuration, the bond between the cation-1 and the anion is parallel to the bond between cation-2 and the anion. The p_σ orbital can be regarded as the p_σ' orbital from the viewpoint of the bond between the anion and cation-2, since the rotation axis of p_σ orbital is parallel to the direction of the bond between the cation-2 and anion. Since the $d\varepsilon'$ orbital is orthogonal to the p_σ' orbital, it follows that the p_σ ($=p_\sigma'$) orbital is orthogonal to the $d\varepsilon'$ for the cation-2.

In contrast, the situation is rather different for the 90° configuration. In this case, the bond between the cation-2 and the anion is perpendicular to the bond between cation-1 and the anion. The p_σ can be regarded as the p_π' orbital from the viewpoint of the bond between the anion and cation-2, since the rotation axis of the p_σ orbital is perpendicular to the direction of the bond between the cation-2 and anion. Since the $d\varepsilon'$ orbital is not orthogonal to the p_π' orbital, then it follows that the p_σ ($=p_\pi'$) orbital is not orthogonal to the $d\varepsilon'$ orbital.

Similar discussion is made for various kinds of superexchange interaction in the 90° and 180° configurations. The rules thus obtained are summarized in the Table for the 90° and 180° configuration.

	90°	180°
$d\varepsilon \perp p_\sigma$	$p_\sigma (=p_\pi') \not\perp d\varepsilon'$	$p_\sigma (=p_\sigma') \perp d\varepsilon'$
$d\gamma \not\perp p_\sigma$	$p_\sigma (=p_\pi') \perp d\gamma'$	$p_\sigma (=p_\sigma') \not\perp d\gamma'$
$d\gamma \perp p_\pi$	$p_\pi (=p_\sigma') \not\perp d\gamma'$	$p_\pi (=p_\pi') \perp d\gamma'$

$$d\varepsilon \not\perp p_\pi \quad p_\pi (= p_\sigma') \perp d\varepsilon' \quad p_\pi (= p_\pi') \not\perp d\varepsilon'$$

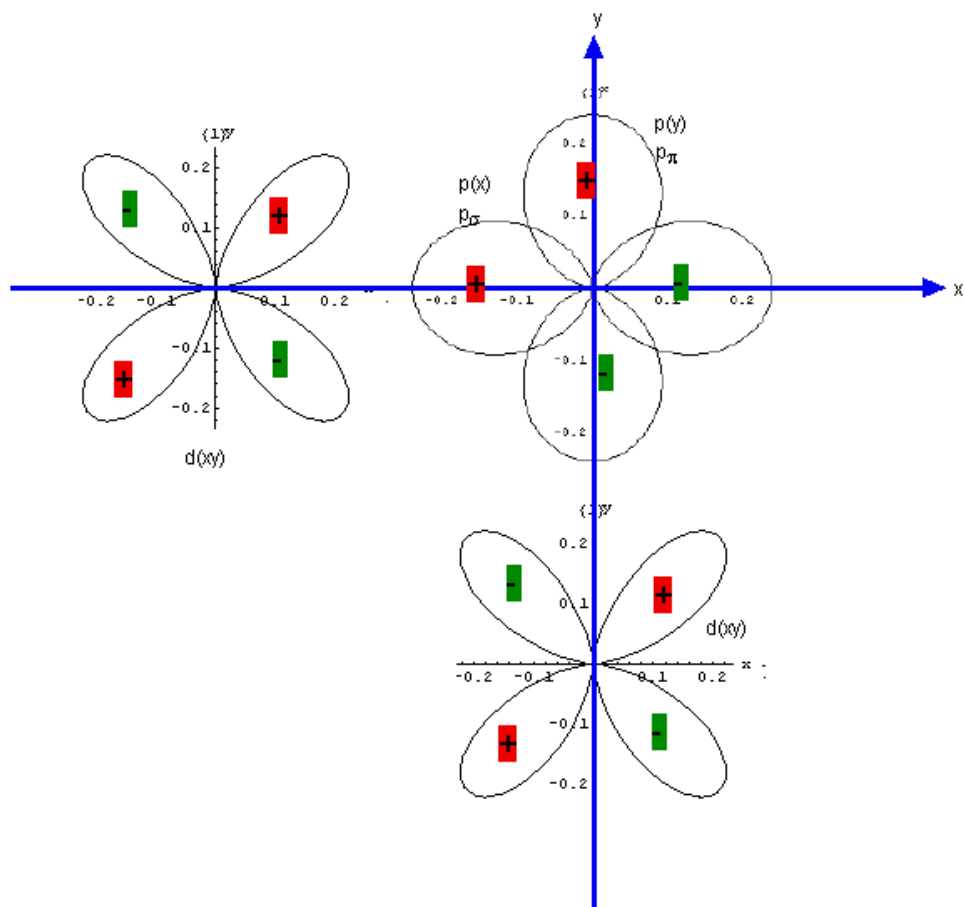


Fig.27 $d\varepsilon \perp p_\sigma$, $p_\sigma (= p_\pi') \not\perp d\varepsilon'$. $d\varepsilon \not\perp p_\pi$, $p_\pi (= p_\sigma') \perp d\varepsilon'$

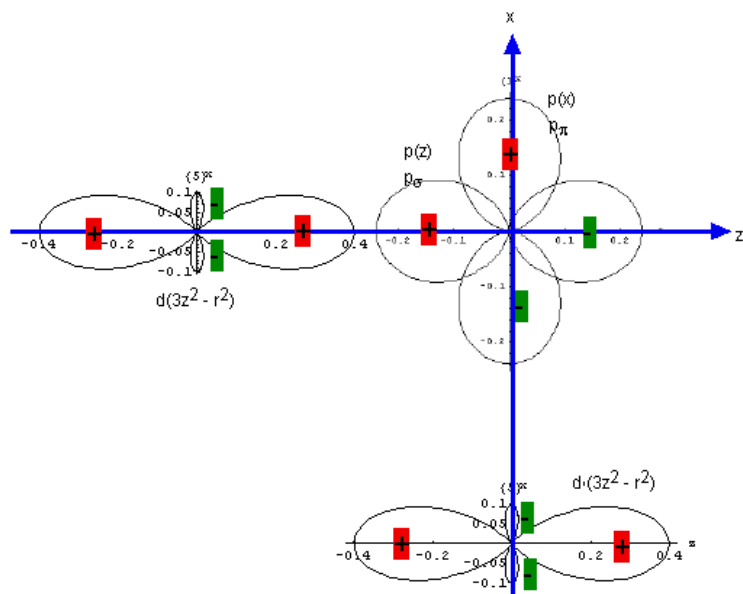


Fig.28 $d\gamma \not\perp p_\sigma$, $p_\sigma (= p_\pi') \perp d\gamma'$. $d\gamma \perp p_\pi$, $p_\pi (= p_\sigma') \not\perp d\gamma'$.

8. Application of GKA rules to real systems

8.1 180° configuration

A. CaMnO₃ 180° case (Kanamori⁸)

In this system, the manganese occurs in the crystal field at the Mn⁴⁺, which means that there are three *d*-electrons: (3*d*)³. The crystal field at the Mn⁴⁺ sites is cubic. Under the effect of a cubic field, the five-fold degenerate orbital *d* state of a single *d* electron is split into an orbital triplet (*d_{xy}*, *t_{2g}*) and an orbital doublet (*d_{yz}*, *e_g*). According to the Hund's rule, the three *d*-electrons will go to one of the *d_{xy}* orbitals with their spins up.

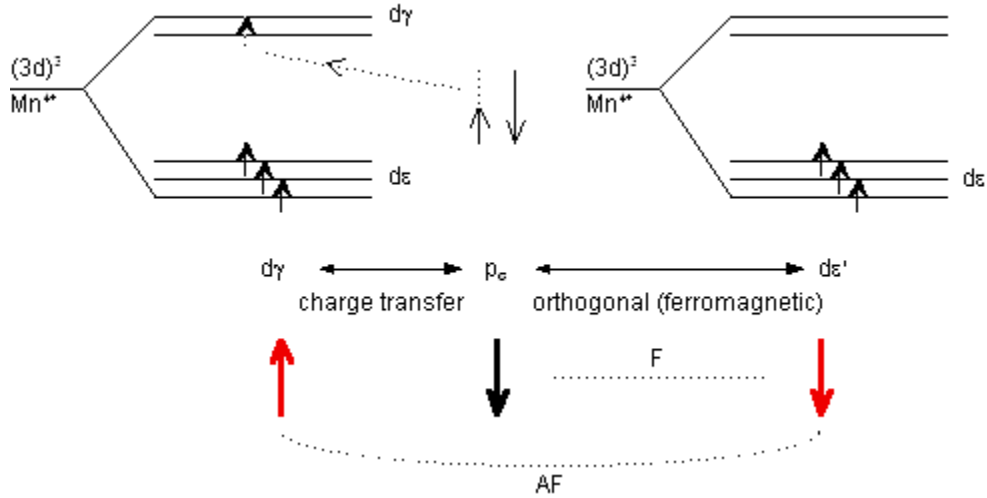


Fig.29 Schematic representation of the superexchange interaction (Mn⁴⁺ - 2*p_σ* - Mn⁴⁺) in the 180° case.

The superexchange involves the *p*-electrons of the O²⁻. The *p*-orbitals are described by *p*(*x*), *p*(*y*), and *p*(*z*), depending on the axis of rotation. These orbitals are classed into two types: (i) the *p_σ* orbital (*p*-orbital whose axis points to one of the cations) and (ii) the *p_π* orbital (*p*-orbital whose axis is perpendicular to the line connecting the anion and cation).

The *p_σ* orbital is orthogonal to the *d*(3*z*² - *r*²), *d*(*xy*), *d*(*yz*), and *d*(*zx*), except for *d*(*x*² - *y*²). A partial covalent bond between the *p_σ* orbital and *d_{xy}* state [*d*(*x*² - *y*²)] can be formed. Then the charge transfer occurs from the *p_σ* orbital with the spin up-state (↑) to the *d_{xy}* state [*d*(*x*² - *y*²)] of the Mn⁴⁺, according to the Hund's rule requiring that the total spin should be maximum. The remaining *p_σ* orbital (spin-down state), which is orthogonal to the *d_{yz}* state, ferromagnetically couples to the *d_{yz}* orbitals of the other Mn⁴⁺. Thus the resultant superexchange interaction between Mn⁴⁺ is antiferromagnetic.

B. NiO, 180° case; (3*d*)⁸

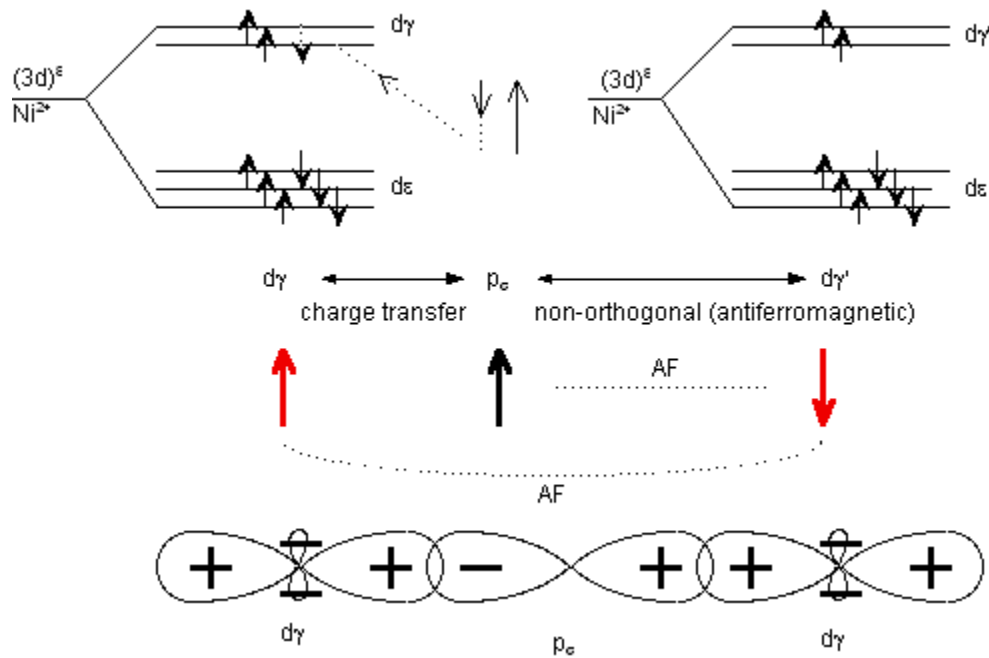


Fig.30 Schematic representation of the superexchange interaction ($\text{Ni}^{2+} - 2p_\sigma - \text{Ni}^{2+}$) in the 180° case.

C. $\text{MnO } 180^\circ$ case

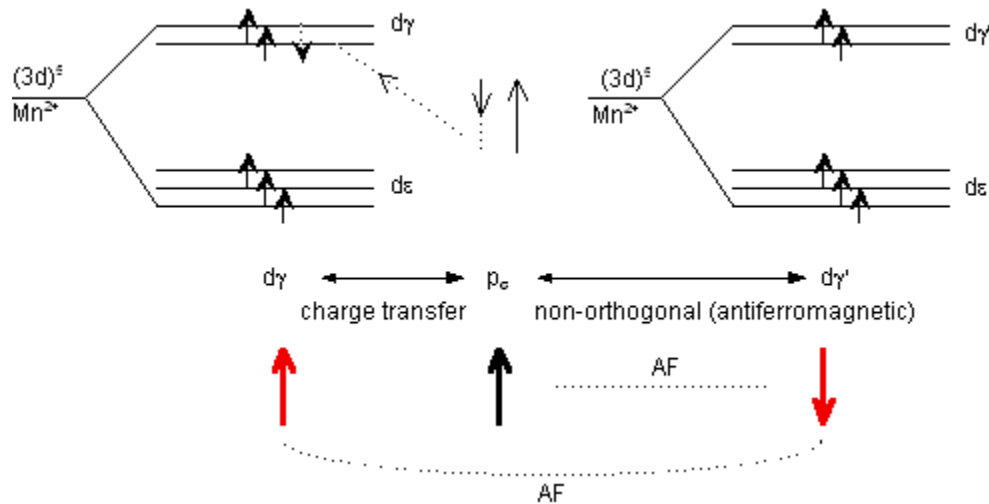


Fig.31 Schematic representation of the superexchange interaction ($\text{Mn}^{2+} - 2p_\sigma - \text{Mn}^{2+}$) in the 180° case.

Note that $d\epsilon - p_\pi$ is very weak.

D. $\text{Ni}^{2+} (3d)^8$ and $\text{V}^{2+} (3d)^3$ 180° case

One can expect a ferromagnetic interaction for this system.

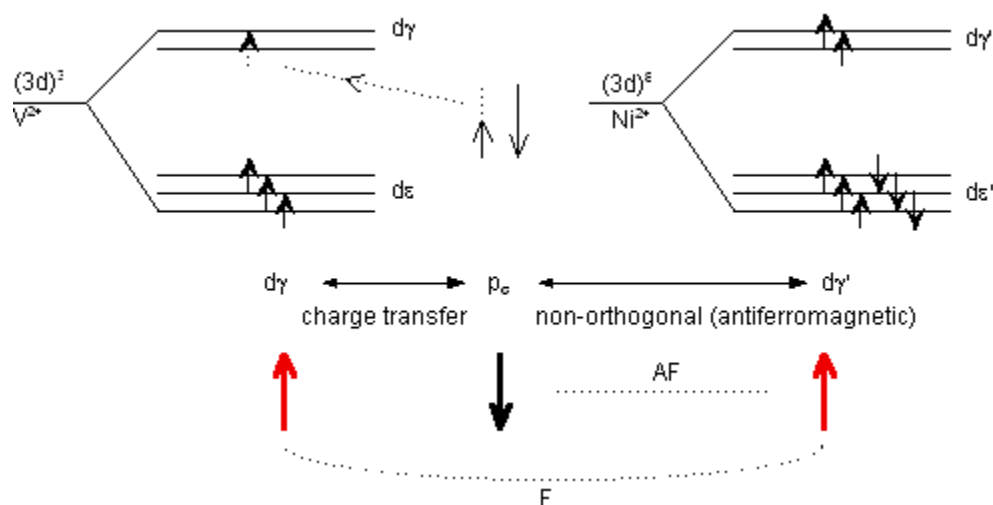


Fig.32 Schematic representation of the superexchange interaction ($V^{2+} - p_{\sigma} - Ni^{2+}$) in the 180° case.

E $Fe^{3+} (3d)^5$ and $Cr^{3+} (3d)^3$ 180° case

(a) One can predict a ferromagnetic interaction.

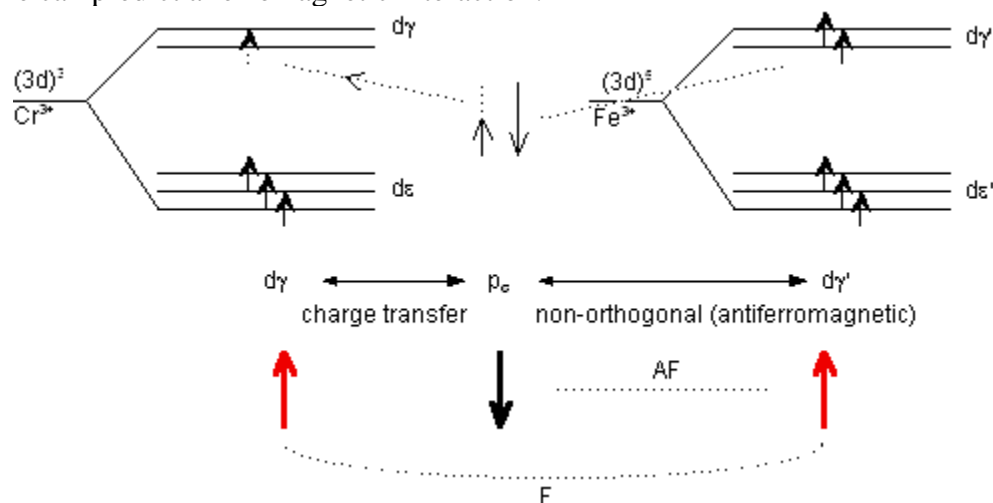


Fig.33 Schematic representation of the superexchange interaction ($Cr^{3+} - p_{\sigma} - Fe^{3+}$) in the 180° case.

(b) The ferromagnetic interaction between Fe^{3+} and Cr^{3+} may be explained by considering that $p_{\sigma}-d\gamma$ bonds are more effective than $d\varepsilon-p_{\pi}$ bonds.

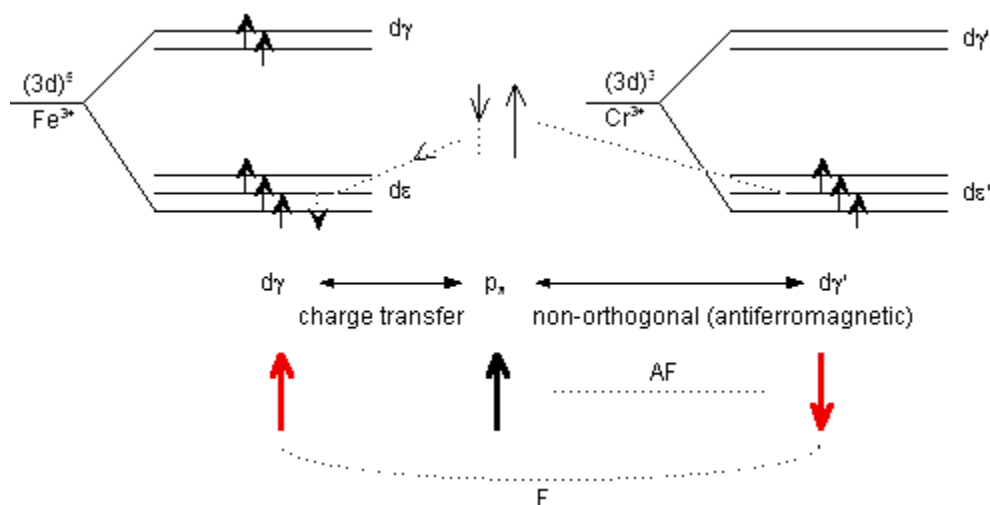


Fig.34 Schematic representation of the superexchange interaction ($\text{Fe}^{3+} - p_{\pi} - \text{Cr}^{3+}$) in the 180° case.

8.2. 90° configuration

A. NiCl_2

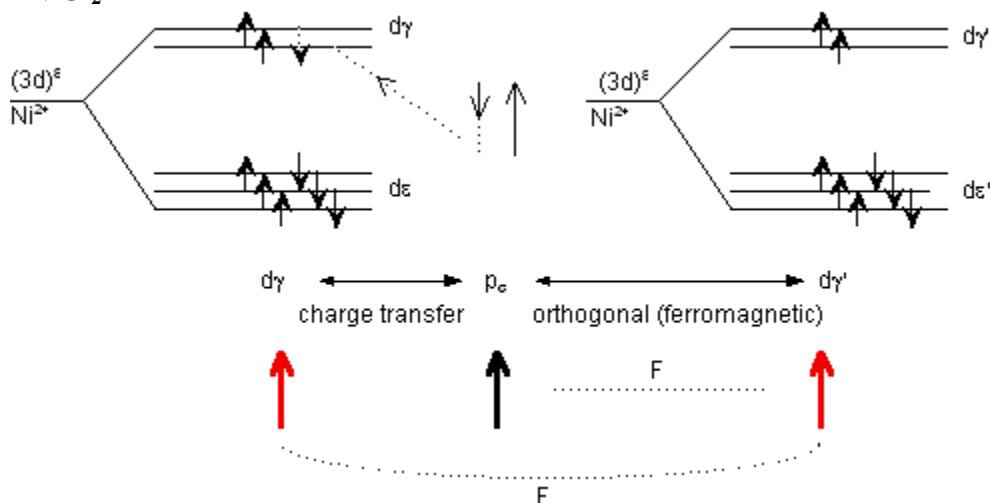


Fig.35 Schematic representation of the superexchange interaction ($\text{Ni}^{2+} - 3p_{\sigma} - \text{Ni}^{2+}$) in the 90° case.

The superexchange involves the p -electrons of the Cl^- . The p_{σ} orbital is orthogonal to the $d(3z^2 - r^2)$, $d(xy)$, $d(yz)$, and $d(zx)$, except for $d(x^2 - y^2)$. A partial covalent bond between the p_{σ} orbital and $d\gamma$ state [$d(x^2 - y^2)$]. can be formed, Then the charge transfer occurs from the p_{σ} orbital with the spin down-state (\downarrow) to the $d\gamma$ state of the Ni^{2+} . The remaining p_{σ} orbital (spin-up state), which is orthogonal to the $d\gamma'$ state, ferromagnetically couples to the $d\gamma'$ orbitals of the other Ni^{2+} . Thus the resultant superexchange interaction between Ni^{2+} is ferromagnetic.

B. CoCl_2

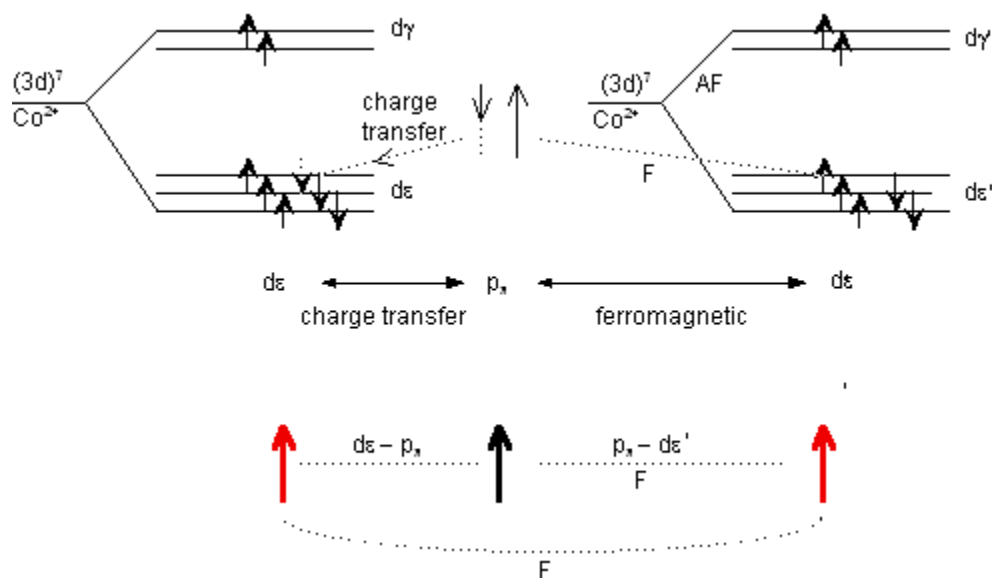


Fig.36 Schematic representation of the superexchange interaction ($\text{Co}^{2+} - 3p_{\pi} - \text{Co}^{2+}$) in the 90° case.

C. CrCl_3

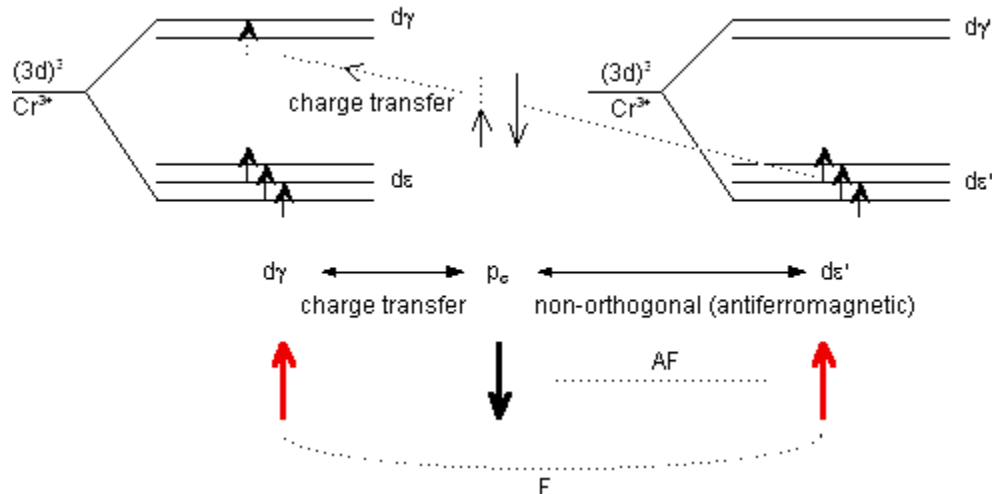


Fig.37 Schematic representation of the superexchange interaction ($\text{Cr}^{3+} - 3p_{\sigma} - \text{Cr}^{3+}$) in the 90° case.

The superexchange involves the p -electrons of the Cl^- ion. The p_{σ} orbital is orthogonal to the $d\gamma$ orbital. A partial covalent bond between the p_{σ} orbital and $d\gamma$ state can be formed. Then the charge transfer occurs from the p_{σ} orbital with the spin up-state (\uparrow) to the $d\gamma$ state of the Cr^{3+} . The remaining p_{σ} orbital (spin-down state), which is orthogonal to the $d\epsilon'$ state, antiferromagnetically couples to the $d\epsilon'$ state of the other Cr^{3+} . Thus the resultant superexchange interaction between Cr^{3+} spins is ferromagnetic.

D. Ni^{2+} and V^{2+} 90° interaction

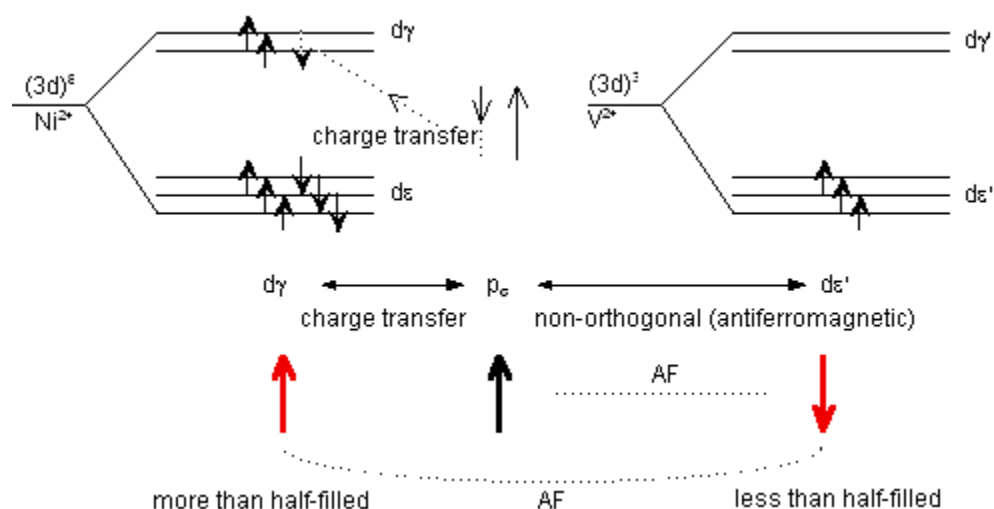


Fig.38 Schematic representation of the superexchange interaction ($\text{Ni}^{2+} - p_\sigma - \text{V}^{2+}$) in the 90° case.

Antiferromagnetic interaction between a cation with a less-than-half-filled d-shell and a cation with a more-than-half-filled d-shell in the 90° case.

E. MnCl_2

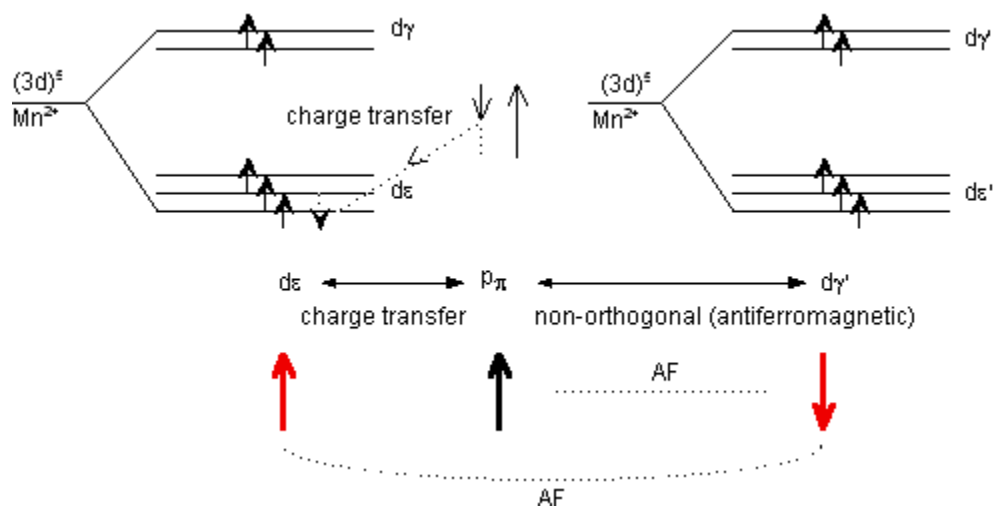


Fig.39 Schematic representation of the superexchange interaction ($\text{Mn}^{2+} - 3p_\pi - \text{Mn}^{2+}$) in the 90° case.

F. CuCl_2

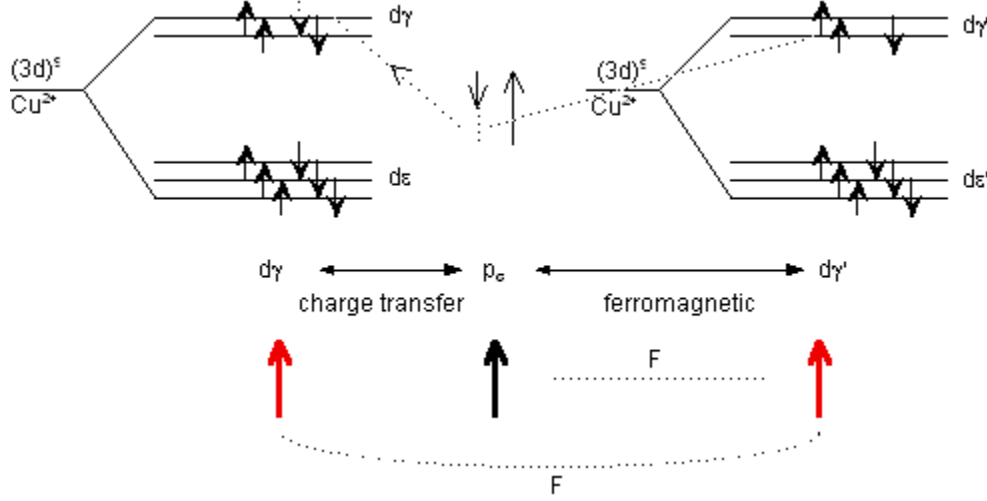


Fig.40 Schematic representation of the superexchange interaction ($\text{Cu}^{2+} - 3p_{\sigma} - \text{Cu}^{2+}$) in the 90° case.

9. Application: La_2CuO_4 as a Mott insulator

Finally we consider a superexchange interaction in La_2CuO_4 which is well-known as a mother-material of high temperature cuprate superconductor (Koike,²¹ 2006). Cu^{2+} ions are located on the square lattice. There is an intervening O^{2-} ion between the nearest neighbor Cu^{2+} ions. Because of the tetragonal crystal field produced by O^{2-} ions and the Jahn-Teller effect related to the spontaneous lattice distortion, the $d\gamma (= \epsilon_g)$ levels are split into the $d(x^2 - y^2)$ level and $d(3z^2 - r^2)$. The $d(x^2 - y^2)$ level (the highest energy level) is occupied by one electron, forming a half-filled band state. Because of the strong electron correlation (Coulomb energy between the electrons with the spin-up state and the spin-down state) in the $d(x^2 - y^2)$ level, the $d(x^2 - y^2)$ level split into the upper Hubbard band and the lower Hubbard band. The lower Hubbard band is fully occupied by one electron, while the upper Hubbard state is empty. Thus the system becomes an insulator. In fact, there is a $2p$ band of O^{2-} between the upper and lower Hubbard band.

Since there are odd numbers of electrons per unit cell, reflecting of $3d^9$ for Cu^{2+} ion it is expected that this system should be a conductor with half-filled state. However, it is really an insulator. This implies that the band theory does not work well in this system. Such an insulator is known as a Mott-Hubbard insulator arising from the strong Coulomb interaction between electrons. When the Coulomb interaction U is much smaller than t , the electrons move over the crystal as a Bloch wave, When U is much larger than t , each electron is localized around the Cu^{2+} ion on the square lattice, leading to the insulator (Sec.3.1).

Magnetically, there exists a superexchange interaction between Cu^{2+} ions through the intervening O^{2-} ion. The mixing of the $d(x^2 - y^2)$ orbital of Cu^{2+} ion and the p_{σ} orbital of O^{2-} ion form a antibonding molecular orbital. Figures 41 and 42 show the electronic density of the antibonding molecular orbitals $|\psi_{ABx}\rangle = |d(x^2 - y^2)\rangle - \lambda|p(x)\rangle$ and $|\psi_{ABy}\rangle = |d(x^2 - y^2)\rangle - \lambda|p(y)\rangle$ with $\lambda = -0.3, 0$, and 0.3 , respectively. The region of one of the clover leaves greatly expands along the $+x$ axis for $|\psi_{ABx}\rangle$ and greatly expands

along the $-y$ axis for $|\psi_{AB_y}\rangle$ for $\lambda = 0.3$. This implies the strong covalency between $d(x^2 - y^2)$ and p_σ along the σ axis where $\sigma = x$ or y . The superexchange interaction leads to the 2D antiferromagnetic correlation between Cu^{2+} spins in the CuO_2 layer. At low temperatures, these CuO_2 planes show a 3D antiferromagnetic long range order through an antiferromagnetic interplanar interaction between the CuO_2 layers.

When holes are doped into La_2CuO_4 , the O^{2-} ions change into O^- ions having electron spins. The antiferromagnetic spin order of Cu^{2+} spins vanishes due to the spin frustration effect from O^- spin between Cu^{2+} ions. In turn, the superconductivity appears. When electrons are doped into La_2CuO_4 , the electrons enter into the upper Hubbard band. The Cu^{2+} ions change into Cu^+ with the electron configuration $(3d)^{10}$. Then the antiferromagnetic order disappears (Koike,²¹ 2006).

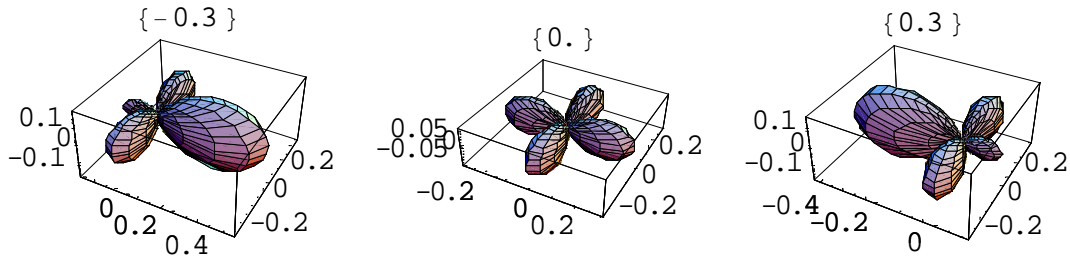


Fig.41 3D polar representation of $|\psi\rangle = |d(x^2 - y^2)\rangle - \lambda|p(x)\rangle$ with $\lambda = -0.3, 0$, and 0.3 .

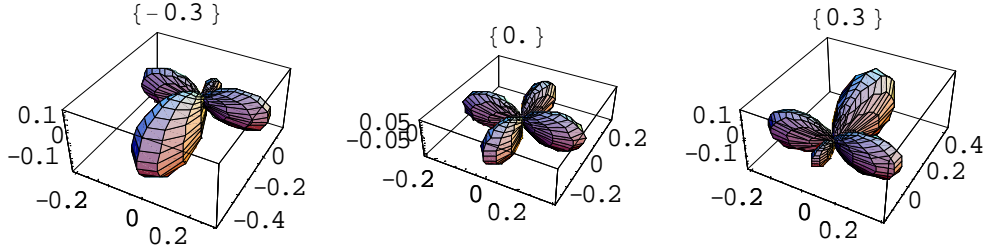


Fig.42 3D polar representation of $|\psi\rangle = |dxy\rangle - \lambda|p(y)\rangle$ with $\lambda = -0.3, 0$, and 0.3 .

10. Conclusion

In 1949, Mott¹⁴ discussed the insulating state and the metal-insulator transition arising from the electron correlation, as an example of NiO. In 1959, Anderson proposed a theory of superexchange interaction. Anderson pointed out that all of insulating magnetic compounds are Mott insulators. The theory not only elucidates the origin of the superexchange interaction but also gives a fundamental basis for the approach of spin Hamiltonian. Thanks to this paper, both the metal state and insulation state can be discussed on the same basis. The high temperature superconductivity is observed in Cu oxides in 1980's. In his proposed theory (1987), Anderson²² claimed that the strong Coulomb interaction (electron correlation) may be responsible for the high T_c superconductivity. It is our current understanding that the high T_c superconductivity is due to the condensation of electron pairs with the symmetry of the d -wave via

antiferromagnetic spin fluctuations based on the superexchange interactions between Cu^{2+} spins.

REFERENCES

1. W. Heisenberg, Z. Phys. **49**, 619 (1928).
2. W. Heitler and F. London, Z. Phys. **44**, 455 (1927).
3. C.G. Shull and J.S. Smart, Phys. Rev. **76**, 1256 (1948).
4. H.A. Kramers, Physica **1**, 182 (1934).
5. P.W. Anderson, Phys. Rev. **79**, 350 (1950).
6. P.W. Anderson, Phys. Rev. **115**, 2 (1959).
7. J.B. Goodenough, Phys. Rev. **100**, 564 (1955).
8. J. Kanamori, J. Phys. Chem. Solid **10**, 87 (1959).
9. P.W. Anderson, Chapter 2 (p.25-83), in *Magnetism*, edited by G.T. Rado and H. Suhl (Academic Press, New York, 1963).
10. J.B. Goodenough, *Magnetism and the Chemical Bond* (Interscience Publisher, New York, 1963).
11. J.J. Sakurai, *Modern Quantum Mechanics Revised Edition* (Addison-Wesley, Reading, MA, 1994).
12. G. Baym, *Lectures on Quantum Mechanics* (W.A. Benjamin, New York, 1969).
13. N.F. Mott and R. Peierls, Proc. Phys. Soc. London **49**, 72 (1937).
14. N.F. Mott, Proc. Phys. Soc. A **62**, 416 (1949).
15. K. Yosida, *Theory of Magnetism* (Springer-Verlag, Berlin, 1996).
16. H. Shiba, *Electron Theory of Solids* (Maruzen, Tokyo 1996). [in Japanese]
17. R.M. White, *Quantum Theory of Magnetism* (Springer-Verlag, Berlin, 2004).
18. J. Kanamori, *Magnetism* (Baifukan, Tokyo, 1969). [in Japanese]
19. L.J. de Jongh and A.R. Miedema, Advances in Physics **50**, 947 (2001).
20. T. Enoki, M. Suzuki, and M. Endo, *Graphite Intercalation Compounds and Applications* (Oxford University Press, New York, 2003).
21. Y. Koike, Materia Japan, **45**, 527 (2006) and **45**, 592 (2006). [in Japanese].
22. P.W. Anderson, Science **235**, 1196 (1987).

Appendix

A. Mathematica program

```
<<Graphics`ParametricPlot3D`
<<Graphics`
SuperStar; expr_* := expr /. {Complex[a_, b_] => Complex[a, -b]}
```

```

ψpx =
-√(1/2) SphericalHarmonicY[1, 1, θ, ϕ] +
√(1/2) SphericalHarmonicY[1, -1, θ, ϕ] // FullSimplify;
ψpy =
i √(1/2)
(SphericalHarmonicY[1, 1, θ, ϕ] + SphericalHarmonicY[1, -1, θ, ϕ]) //
FullSimplify; ψpz = SphericalHarmonicY[1, 0, θ, ϕ] // FullSimplify;
ψdxy =
-i √(1/2)
(SphericalHarmonicY[2, 2, θ, ϕ] - SphericalHarmonicY[2, -2, θ, ϕ]) //
FullSimplify;
ψdyz =
i √(1/2)
(SphericalHarmonicY[2, 1, θ, ϕ] + SphericalHarmonicY[2, -1, θ, ϕ]) //
FullSimplify;
ψdzx =
-√(1/2)
(SphericalHarmonicY[2, 1, θ, ϕ] - SphericalHarmonicY[2, -1, θ, ϕ]) //
FullSimplify;
ψdx2y2 =
√(1/2) (SphericalHarmonicY[2, 2, θ, ϕ] +
SphericalHarmonicY[2, -2, θ, ϕ]) // FullSimplify;
ψd3z2r2 = SphericalHarmonicY[2, 0, θ, ϕ] // Simplify;
Ad5p3[k_] := Abs[ψd3z2r2 - k ψpz]2 // Simplify;
Ad5p1[k_] := Abs[ψd3z2r2 - k ψpx]2 // Simplify;
Adzxp3[k_] := Abs[ψdzx - k ψpz]2 // Simplify;
Adzxp1[k_] := Abs[ψdzx - k ψpx]2 // Simplify;

Qt1[k_] := SphericalPlot3D[Evaluate[Ad5p3[k]], {θ, 0, π}, {ϕ, 0, 2π},
PlotLabel → {k}, PlotPoints → 40, PlotRange → All, DisplayFunction →
Identity]; Rt1[k_] := SphericalPlot3D[Evaluate[Ad5p1[k]], {θ, 0, π},
{ϕ, 0, 2π}, PlotLabel → {k}, PlotPoints → 40, PlotRange → All, DisplayFunction →
Identity]; St1[k_] := SphericalPlot3D[Evaluate[Adzxp3[k]], {θ, 0, π}, {ϕ, 0, 2π},
PlotLabel → {k}, PlotPoints → 40, PlotRange → All, DisplayFunction →
Identity]; Tt1[k_] := SphericalPlot3D[Ev

```

```

valuate[Adzxp1[k]], { $\theta$ , 0,  $\pi$ }, { $\phi$ , 0,  $2\pi$ }, PlotLabel -> {k}, PlotPoints
->40, PlotRange -> All, DisplayFunction -> Identity]

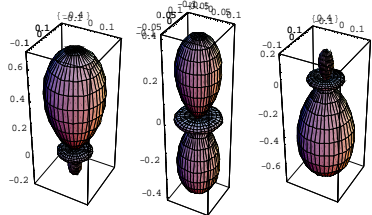
```

(a) Mixing of $d(3z^2-r^2)$ and $p(z)$ orbitals, $d(3z^2-r^2) - k p(z)$. k is changed as a parameter. $p(z)$ is a $p\sigma$ orbital.

```

Qt2=Table[Qt1[k], {k, -
0.4, 0.4, 0.4}]; Qt3=Show[GraphicsArray[Partition[Qt2, 3]], Displ
ayFunction -> $DisplayFunction]

```



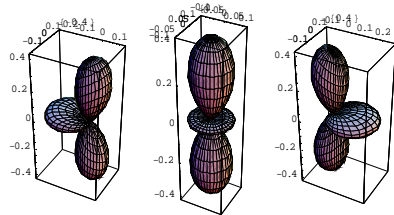
-GraphicsArray-

(b) Mixing of $d(3z^2-r^2)$ and $p(x)$ orbitals, $d(3z^2-r^2) - k p(x)$. k is changed as a parameter. $p(x)$ is a $p\pi$ orbital.

```

Rt2=Table[Rt1[k], {k, -
0.4, 0.4, 0.4}]; Rt3=Show[GraphicsArray[Partition[Rt2, 3]], Displ
ayFunction -> $DisplayFunction]

```



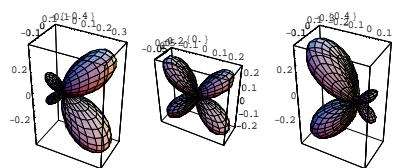
-GraphicsArray-

(c) Mixing of $d(zx)$ and $p(z)$ orbitals, $d(zx) - k p(z)$. k is changed as a parameter. $p(z)$ is a $p\sigma$ orbital.

```

St2=Table[St1[k], {k, -
0.4, 0.4, 0.4}]; St3=Show[GraphicsArray[Partition[St2, 3]], Displ
ayFunction -> $DisplayFunction]

```



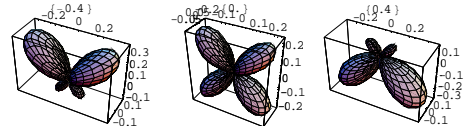
-GraphicsArray-

(d) Mixing of $d(zx)$ and $p(x)$ orbitals, $d(zx) - k p(x)$. k is changed as a parameter. $p(x)$ is a $p\pi$ orbital.

```

Tt2=Table[Tt1[k], {k, -
0.4, 0.4, 0.4}]; Tt3=Show[GraphicsArray[Partition[Tt2, 3]], Displ
ayFunction -> $DisplayFunction]

```



-GraphicsArray-

B. Magnetic properties of typical magnetic compounds

The magnetic properties of pure compounds and graphite intercalation compounds (GICs) (quasi 2D spin systems) are obtained from the Ref.19 and Ref.20, respectively.

FeTiO₃

Ilmenite structure. An Ising antiferromagnet with the easy direction of spins along the c -axis. The Fe ions on the hexagonal lattice are ferromagnetically ordered. The 2D ferromagnetic layers are stacked along the c axis. $T_N = 58.0$ K. $|J'/J| = 0.2$.

MnTiO₃

Ilmenite structure. An Ising antiferromagnet with the easy direction of spins along the c -axis. The Mn ions on the hexagonal lattice are antiferromagnetically ordered. $T_N = 63.6$ K. $|J'/J| = 0.04$.

K₂MnF₄

K₂NiF₄ type structure. $a = 4.20$ Å. $c = 13.14$ Å. Antiferromagnet. $T_N = 42.37$ (58.0) K. Spin// c . Typical 2D antiferromagnet.

K₂CoF₄

K₂NiF₄ type structure. 2D Ising antiferromagnet. Spin// c . $T_N = 107$ K. $S = 1/2$ (fictitious spin)
 $g_c = 6.30$. $g_a = 3.13$.

K₂NiF₄

$a = 4.006$ Å. $c = 13.076$ Å. 2D antiferromagnet. $T_N = 97.1$ K. Spin// c . Typical 2D antiferromagnet.

K₂CuF₄

K₂NiF₄ type structure. $a = 4.155$ Å. $c = 12.71$ Å. 2D Heisenberg-like Ferromagnet with XY spin anisotropy. $T_c = 6.25$ K. Spin $\perp c$. $S = 1/2$. $J = 11.2$ K. $H_A = 2.44$ kOe. Typical 2D XY-like ferromagnet.

MnCl₂

CdCl₂ type structure, $a = 6.20$ Å, $\alpha = 33^\circ 33'$. Antiferromagnet. $T_{N1} = 1.96$ K and $T_{N2} = 1.81$ K. Spin $\perp c$. Complicated magnetic structure (neutron scattering). Two peaks of λ -type in the heat capacity.

FeCl₂

CdCl₂ type structure. $a = 6.20$ Å. $\alpha = 33^\circ 33'$. Antiferromagnet. spin direction // c , $T_N = 23.5$ K. Ferromagnetic intraplanar exchange interaction ($J = 3.4$ K). antiferromagnetic interplanar exchange interaction. Metamagnetism. $H_e = 11.6$ kOe, $H_A = 43$ kOe, $H_E = 140$ kOe. Fictitious spin $S = 1$.

CoCl₂

CdCl₂ type structure. $a = 6.16$ Å. $\alpha = 33^\circ 33'$. Antiferromagnet. $T_N = 24.7$ K. Intraplanar ferromagnetic and interplanar antiferromagnetic exchange interactions. Spin $\perp c$. XY-like spin anisotropy. $g_c = 3.04$. $g_a = 4.95$. $S = 1/2$ (fictitious spin). $J_1 = 10.4$ K. $J_2 = -0.89$ K.

NiCl₂

CdCl₂ type structure. $a = 6.13$ Å. $\alpha = 33^\circ 36'$. Antiferromagnet. $S = 1$. $T_N = 52$ K. Intraplanar ferromagnetic and interplanar antiferromagnetic exchange interactions. Spin $\perp c$. XY-like spin anisotropy. $J_1 = 9.5$ K. $J_2 = -0.73$ K.

CrCl₃

- $a = 5.942 \text{ \AA}$. $c = 17.333 \text{ \AA}$. Antiferromagnet. $T_N = 16.8 \text{ K}$. Intraplanar ferromagnetic and interplanar antiferromagnetic exchange interactions. Spin $\perp c$. Transition from antiferromagnetic phase to the ferromagnetic phase occurs only at H_c (= several kOe).
- FeCl₃
 $a = 6.065 \text{ \AA}$. $c = 17.44 \text{ \AA}$. Antiferromagnet. $T_N = 15 \text{ K}$. spin spiral in the (14 $\bar{5}$ 0) plane. The rotation angle is $2\pi/15$ per layer.
- Stage-2 CrCl₃ GIC
 Quasi 2D XY-like ferromagnet on the hexagonal lattice. $T_{cu} = 11.5 \text{ K}$. $T_{cl} = 10.3 - 10.5$. $c = 12.80 \text{ \AA}$. The intraplanar interaction is ferromagnetic ($J = 5.86 \text{ K}$). The interplanar interaction is very weak and antiferromagnetic. $S = 3/2$.
- Stage-2 FeCl₃ GIC
 Quasi 2D antiferromagnet on the hexagonal lattice. Spin glass like transitions at $T_{SG}^{(h)} = 4.5 \text{ K}$. $T_{SG}^{(l)} = 2 \text{ K}$. The FeCl₃ layers may be formed of majority Fe³⁺ spins with XY spin anisotropy and minority Fe²⁺ spins with Ising anisotropy. The intraplanar exchange interaction between Fe³⁺ spins is antiferromagnetic. $S = 5/2$.
- Stage-2 MnCl₂ GIC
 Quasi 2D Heisenberg-like antiferromagnet on the triangular lattice. $S = 5/2$. $T_N = 1.1 \text{ K}$. No magnetic phase transition is observed from neutron scattering.
- Stage-2 CoCl₂ GIC
 Quasi 2D XY-like ferromagnet. $T_{cu} = 8.9 \text{ K}$. $T_{cl} = 6.9 \text{ K}$. Fictitious spin $S = 1/2$. The interplanar exchange interaction is antiferromagnetic, while the intraplanar exchange interaction is ferromagnetic ($J = 7.75 \text{ K}$). The anisotropic exchange interaction J_A is 3.72 K .
- Stage-2 NiCl₂ GIC
 Quasi 2D XY-like ferromagnet on the triangular lattice. $T_{cu} = 21.3 \text{ K}$. $T_{cl} = 18 \text{ K}$. Spin $S = 1$. The interplanar exchange interaction is antiferromagnetic, while the intraplanar exchange interaction is ferromagnetic ($J = 7.5 \text{ K}$).
- Stage-2 CuCl₂ GIC
 Quasi 2D Heisenberg-like antiferromagnet on the isosceles triangle. No magnetic phase transition is observed from magnetic neutron scattering. The DC magnetic susceptibility shows a broad peak at $62 - 65 \text{ K}$. $S = 1/2$.